FRONTOGENETICAL PROCESSES IN THE UPPER TROPOSPHERE

by

KENNETH ARTHUR CAMPANA
A.B., Boston University
(1963)

Submitted in partial fulfillment of the requirements
for the degree of Master of Science at the
MASSACHUSETTS INSTITUTE OF TECHNOLOGY

July 1965

Signature of Author . . . . . .
Department of Meteorology, July 1965

Certified by. . . . . .
Thesis Supervisor

Accepted by . . . . . .
Chairman, Departmental Committee on
Graduate Students

FRONTOGENETICAL PROCESSES IN THE UPPER TROPOSPHERE

by
KENNETH ARTHUR CAMPANA

Submitted to the Department of Meteorology on July 20, 1965 in partial fulfillment of the requirement for the degree of Master of Science.

ABSTRACT

An intense upper-tropospheric front located over the southeastern United States on 20 February 1964 is examined in the horizontal and vertical planes. Due to the extreme dryness of the region, the adiabatic assumption is considered valid. Trajectories ending in the baroclinic zone are constructed using a total energy equation and conservation of potential vorticity as guides. Then a study of the change in frontal intensity in the horizontal is made.

The rapid intensification of the front is not coincident with any surface deepening, but appears to occur with a marked increase in horizontal confluence. The baroclinic zone crosses the 500-mb level beneath the jet core and extends below 700 mb, but it is not associated with any surface front. Air is descending throughout the region, and an indirect circulation is noted everywhere except at 600 mb. The trajectories and high potential vorticity values lend support to a stratospheric origin for the air parcels in the front. Potential vorticity increases along the trajectories at the higher isentropes through most of the frontal zone, and this is attributed to diabatic effects rather than to frictional torques.

Both horizontal confluence and vertical tilting effects are present in the rapid frontogenesis; and it is suggested that the former predominates in the frontal zone and the latter predominates at the entrance to the front.

Thesis Supervisor: Frederick Sanders
Title: Associate Professor

ACKNOWLEDGEMENT

There have been several persons that I wish to thank for aiding me in the completion of this thesis. My thanks to Mrs. Jane McNabb and Miss Penny Freeman for typing the paper and for the production of the necessary copies. A few fruitful discussions with fellow student, Mike Wallace, were of great aid to me in beginning the trajectory analyses.

Without the help of Miss Isabelle Kole, who instructed me in the use of drafting equipment, the accompanying diagrams would not have been done. My thanks also to her for taking time to prepare the more difficult diagrams.

I reserve special thanks for Professor Frederick Sanders whose invaluable discussions with me and whose helpful suggestions have made this thesis possible.

TABLE OF CONTENTS

I.	INTRODUCTION		1
	A. Historical Background	1	
	B. Importance of High-Level Fronts	3	
II.	THEORY BASIC TO CONSTRUCTION OF TRAJECTORIES		6
	A. First Law of Thermodynamics	6	
	B. Montgomery Stream Function	7	
	C. Total Energy Equation	7	
	D. Potential Vorticity	10	
III.	SYNOPTIC SITUATION: 18-20 February 1964		17
IV.	METHODS OF LOCATING THE FRONT		19
	A. Plotting Radiosonde Data	19	
	B. Potential Temperature Analyses	21	
	C. Potential Temperature Cross Section Analyses	24	
V.	DISCUSSION OF RESULTS		28
	A. Trajectories	28	
	B. Conservation of Potential Vorticity	30	
	C. Stratospheric Origin of Trajectories	34	
	D. Frontogenesis in the Thermal Field	37	
VI.	CONCLUSIONS		42
	APPENDICES		44
	Figures 1 - 37		46
	BIBLIOGRAPHY		83

I. INTRODUCTION

A. Historical Background

Man has looked at the sky for centuries and has observed phenomena existing far from the earth. The stars and the motions of planets were two of the features that drew his attention upward. Early in the twentieth century man again looked toward the sky, not for extra-terrestrial purposes, but to observe the characteristics of weather patterns. Before 1920, Bjerknes (1919) postulated the existence of weather fronts simply from observations. A front was defined as a sloping boundary between adjacent and differing air masses. Margules had developed a theory of fronts, using geostrophic and hydrostatic conditions, just after the turn of the century, but for the first time surface observations were bearing out their existence. Bjerknes postulated the existence of a steering line (warm front) and of a squall line (cold front), the classification depending upon which air mass was advancing into a region.

This was the start of the Norwegian school in early meteorology. Later Bjerknes and Solberg (1921, 1922) used empirical results to develop the polar front and wave cyclone theories. In all these cases a front was thought to be a sharp discontinuity in temperature. Eventually vast amounts of surface and upper-air data showed that fronts were not sharp boundaries, rather they were often broad zones of transition. Although intense baroclinic

regions near the ground can be considered as temperature discontinuities, those zones found above the friction layer are mainly discontinuities of temperature gradient. Many persons became skeptical of the polar front theory when these broad transition zones were found, and theoretical meteorologists have abandoned them completely in their dynamical models. The role of the front has decreased in modern meteorology as the theoretical branch has increased, but nevertheless fronts are still basic to the weather forecaster.

Sanders (1954) has discussed two types of frontal zones. One type is the surface front which reaches its maximum intensity near the ground and becomes rather diffuse above 700 mb. In this case warm air is forced to rise due to the presence of denser cold air, and extensive cloudiness and precipitation usually result. With the advent of a widespread radiosonde network, another class of fronts was found—the middle and high tropospheric type. Palmén (1948) noted that these fronts were found well above 700 mb and often crossed the 500 mb level vertically below the jet stream. Sanders has found them to be different from a mere extension of surface fronts. They seem to be manifestations of subsiding masses of air and reach their maximum intensity near 500 mb. Evidence has been obtained that suggests a thermally indirect circulation near these zones. This is the type of front with which we shall be concerned; and it is characterized by strong vertical wind shear, by pronounced temperature gradient, and by high stability and vorticity values.

B. Importance of High-Level Fronts

It must be made clear at the start that these high tropospheric fronts are not rare occurrences. They are often found on the western sides of vigorous atmospheric disturbances and initially are located near the tropopause. As the storm matures, the frontal zone appears to descend and to move in the direction of air flow. During this time, the jet intensifies and air parcels flowing through the baroclinic zone are continually subjected to frontogenetical and frontolytical processes. As the front moves to the south and southeast sides of the trough, it attains strong intensity near the 500-mb or 600-mb levels. At no time in the history of one of these fronts does it seem to be a mere extension of a surface front.

One of the prime reasons for studying these transition zones is to confirm or to deny the existence (in these fronts) of a mode of mass exchange between the stratosphere and troposphere. By tracing back in time air parcels that constitute several of these fronts, Staley in 1960 and Danielsen in 1964 have shown that there is often air of stratospheric origin in these zones. Air mass exchange of this type is important in modern studies of atmospheric motions and high-level radioactivity.

The mechanics of the general circulation of the atmosphere is a problem that has long confronted earth scientists. Meridional air motions have been postulated since the time of Hadley in the seventeenth century. Recently, several studies, including those

of Newell (1963) and Oort (1963), have been made using ozone as a tracer, and it seems that three meridional cells exist. A thermally direct (warm air rising) cell exists in the tropics and a thermally indirect cell exists in middle latitudes, but the expected cell in the polar regions has been difficult to observe. High-level frontogenesis may simply be a manifestation of the air exchange between stratosphere and troposphere that is necessary for the existence of these cells.

Since the advent of nuclear testing, movement of air through the tropopause has been given more attention. Radioactivity that is injected into the stratosphere must pass into the troposphere before it eventually reaches the earth's surface. Danielsen (1964) and others have found high concentrations of nuclear debris in these high-level fronts, and thus further proof of air mass exchange via these zones is established.

Another important reason for studying these fronts is the existence of clear air turbulence (CAT) associated with the strong vertical wind shear. It is difficult to assess the various atmospheric parameters in relation to turbulent processes, but it seems that a knowledge of these high-level fronts could be of assistance in determining regions of CAT.

A final possibility for examining these high baroclinic zones is simply to compare them with surface fronts.

Thus we see that the field of frontal study is still quite active, and although this investigation will not delve into all of

the above problems, it will add another case study to the record. There are three general roads that we shall follow. First, a description of the temperature structure of the front will be made in the horizontal and the vertical planes, while its evolution in time and space is being displayed. Second, the possible stratospheric origin of the air in the frontal zone will be examined. Finally, the characteristics of the frontogenetical and frontolytical effects induced by the accompanying motion field will be studied.

Before we can begin to investigate the specific case in February 1964, the theory behind the construction of air parcel trajectories, which will be important in the second objective of this thesis, is presented. Most of the techniques for attaining the first and third objectives are basic enough to the reader so that they may be employed with little explanation in the text.

II. THEORY BASIC TO CONSTRUCTION OF TRAJECTORIES

A. First Law of Thermodynamics

If one assumes that the atmosphere is an inviscid fluid, the only work that can be done is expansion against the pressure forces. Therefore an amount of heat, dQ, added to a unit mass of air must balance both the internal energy ($c_v dT$) and the work done ($p d\alpha$),

$$dQ = c_v dT + p d\alpha \tag{1}$$

where c_v is the specific heat of air at constant volume, T is the temperature, p is the pressure, and α is the specific volume. Note that dQ is not an exact differential. By making use of the equation of state for a perfect gas, the First Law of Thermodynamics for adiabatic flow becomes:

$$\frac{d\theta}{dt} = 0 \tag{2}$$

This implies that the potential temperature is conserved if one follows an air parcel. In our case, the front is located in a very dry region far enough from the surface of the earth and from layers of heat absorbing or heat radiating clouds that the adiabatic assumption is valid. Although low cloudiness exists below the northernmost portions of the zone on the final day, we shall assume it is a sufficient distance under the region of interest that adiabatic motion still holds. Thus, isentropic flow will be our first constraint on the trajectories.

B. Montgomery Stream Function

The geostropic wind field on an isentropic surface (Appendix I) will be depicted by analyzing values of the Montgomery stream function, ψ ,

$$\psi = c_p T_\theta + g Z_\theta \qquad (3)$$

where c_p is the specific heat of air at constant pressure, g is the acceleration of gravity, T_θ and Z_θ are the temperature and height of the specific surface. As Danielsen (1958) shows, ψ , must be known to four significant figures if the geostrophic wind is to be reliably determined. This means the temperature must be known to tenths of a degree and height to tens of meters, which seems impossible. However, as Danielsen further shows, ψ can be calculated with little error depending on the accuracy with which we know the pressure of the isentropic surface. If T_θ and p_θ are determined independently, then large errors may result; however, when Poisson's equation is used to obtain one from the other, the error is found to be small up into the middle atmosphere. This latter operation has been performed in the computation of ψ for our case, so it seems the errors involved will not invalidate the stream function analysis.

C. Total Energy Equation

A first approximation to the initial locations of trajectories ending in the frontal zone is the following kinematic relation:

$$D = \frac{V_1 + V_2}{2} \Delta t \qquad (4)$$

Here D is the distance traversed, V_1 is the velocity used in the first time period, V_2 is the velocity used in the second time period, and Δt is the time difference between the initial and final points. Since a twelve-hour time interval is involved, one traces the path backwards along the ψ- field for the last six-hour period and then along the ψ - field for the first six-hour period. In our case study, the geostrophic direction of flow and the actual wind speeds (which were sub-geostrophic) have been used in conjunction with (4).

To improve the accuracy of the trajectory obtained by (4), an equation is developed below which accounts for the change in kinetic energy of the parcel by giving it a deviation from its geostrophic path. If the parcel simply follows the ψ- lines for the two time periods, it may start with a velocity of forty knots, but it may end with a velocity of eighty knots. The increase in velocity is a result of the horizontal pressure-gradient force acting on a parcel which has a non-geostrophic path, and in the example above the increase is accounted for if the initial point is at a higher ψ-value than the final point.

Now let us look at the simple definition of the total derivative of ψ, using x, y, θ as co-ordinates,

$$\frac{d\psi}{dt} = \frac{\partial \psi}{\partial t} + \vec{v} \cdot \nabla \psi + \frac{d\theta}{dt} \frac{\partial \psi}{\partial \theta} \qquad (5)$$

In this system $\frac{d\theta}{dt}$ is like the vertical velocity, since $\vec{v}$ is

the horizontal velocity. In our case the last term on the right is zero. On an isentropic surface, the vector equation of horizontal, frictionless motion is written as follows:

$$\frac{d\vec{v}}{dt} = -\nabla\psi - f(\hat{k} \times \vec{v}) \qquad (6)$$

where $\hat{k}$ is the unit vector in the vertical direction. Now take the dot product of $\vec{v}$ with equation (6), and get

$$\frac{d}{dt}\left(\frac{|\vec{v}|^2}{2}\right) = -\vec{v} \cdot \nabla\psi \qquad (7)$$

Adding (5) and (7),

$$\frac{d}{dt}\left(\psi + \frac{V^2}{2}\right) = \frac{\partial\psi}{\partial t} \qquad (8)$$

where $|\vec{v}|^2 \equiv V^2$

The term on the left-hand side is a measure of the energy of an air parcel, since ψ is a sum of internal and potential energies and $V^2/2$ is the kinetic energy. The term on the right-hand side is the change in the ψ-field at a fixed point. Now integrate (8) with respect to time over the length of the trajectory,

$$\psi_f - \psi_i + \frac{V_f^2}{2} - \frac{V_i^2}{2} = \int_f^i \frac{\partial\psi}{\partial t}\, dt \qquad (9)$$

where $(\,)_f$ is at the final time and $(\,)_i$ is at the initial time. The integral on the right can be approximated by the twelve-hour difference in ψ at the initial, middle and final points of the

trajectory. These values are found by graphical subtraction of the ψ-analyses. Therefore, an equation which can be called a total energy equation, has been developed to help us obtain more accurate trajectories

$$\psi_f - \psi_i + \frac{V_f^2}{2} - \frac{V_i^2}{2} \simeq \frac{\Delta\psi_f + \Delta\psi_i + 2\Delta\psi_M}{4} \qquad (10)$$

Here, Δ implies a twelve-hour change and $(\ )_M$ is the value at the middle point of the particle path. Equation (10) is a means of measuring cross-contour flow, which implies that work is being done on the parcel by the environment or vice versa. In applying this equation to the present study, it is found the ψ-field varies so much in space that ψ_i is constrained to a narrow region on an isentropic surface. Since most of the air parcels in our case study are being accelerated in time, suppose as an example, we place a final point in the jet stream. By using (4), a first approximation to the initial point is determined; however, ψ_i will not satisfy (10) because it is so low. By moving the initial point towards higher ψ-values, (10) is satisfied, as is (4), and the air parcel curves more anticyclonically than the ψ-field, from higher to lower values of the stream function.

D. Potential Vorticity

There is still another means of determining a more accurate trajectory; that is by the conservation of potential vorticity. The theory behind this quantity is developed below[1]. The theorem

---

1. The proof is due in part to notes obtained in course 18.634 at M.I.T., taught by Pedlosky.

will be proven for the standard x, y, z co-ordinate system and then will be transformed into an equation on an isentropic surface.

The vector equation of motion for the earth's atmosphere may be written as follows:

$$\frac{\partial \vec{v}}{\partial t} + \vec{v} \cdot \nabla \vec{v} + (\vec{f} \times \vec{v}) = -\frac{\nabla p}{\rho} - g\hat{k} + \vec{F} \qquad (11)$$

where $\hat{k}$ is the unit vector in the local vertical direction, g is the acceleration due to gravity, $\vec{F}$ is some frictional force vector, and $\vec{f}$ is the earth's rotational vector.

Now substitute the following identity

$$\vec{v} \cdot \nabla \vec{v} \equiv \nabla \frac{|\vec{v}|^2}{2} - \vec{v} \times curl \vec{v} = \nabla \frac{|\vec{v}|^2}{2} - \vec{v} \times \vec{\omega} \qquad (12)$$

into (11) and take the curl of the resulting equation to get

$$\frac{\partial \vec{\omega}}{\partial t} + \nabla \times \left[(\vec{\omega} + \vec{f}) \times \vec{v} \right] = \frac{\nabla \rho \times \nabla p}{\rho^2} + \nabla \times \vec{F} \qquad (13)$$

Here $\vec{\omega}$ is the three-dimensional vorticity vector. We have also made use of the fact that $g = |\nabla \Phi|$ and

$$\nabla \times \nabla (\ ) = 0 \qquad (14)$$

$\nabla \Phi$ is the apparent gravitational potential, which is directed normal to the geoid. We take the following identity,

$$\nabla \times \left[(\vec{\omega} + \vec{f}) \times \vec{v} \right] = \vec{v} \cdot \nabla (\vec{\omega} + \vec{f}) - (\vec{\omega} + \vec{f}) \cdot \nabla \vec{v} + (\vec{\omega} + \vec{f})(\nabla \cdot \vec{v}) - \vec{v}(\nabla \cdot (\vec{\omega} + \vec{f})) \qquad (15)$$

and substitute it into (13). Noting that the last term on the right of (13) is zero, we obtain,

$$\frac{d}{dt}(\vec{\omega}+\vec{f}) = (\vec{\omega}+\vec{f})\cdot\nabla\vec{v} - (\vec{\omega}+\vec{f})(\nabla\cdot\vec{v}) + \frac{\nabla\rho\times\nabla p}{\rho^2} + \nabla\times\vec{F} \tag{16}$$

This is the Helmholtz vorticity theorem. It is not a conservation equation, but it does tell us the vorticity of a particle can change by tipping the vorticity vector, by three dimensional divergence of the air motion, by a baroclinic effect, or by frictional torque. The continuity equation (17) is used to simplify (16).

$$\nabla\cdot\vec{v} = -\frac{1}{\rho}\frac{d\rho}{dt} \tag{17}$$

Now take the dot product of $\nabla\theta$ and the Helmholtz equation (16), and get

$$\nabla\theta\cdot\frac{d}{dt}(\vec{\omega}+\vec{f}) - \frac{1}{\rho}\frac{d\rho}{dt}\nabla\theta\cdot(\vec{\omega}+\vec{f}) =$$

$$= \nabla\theta\cdot\frac{\nabla\rho\times\nabla p}{\rho^2} + \nabla\theta\cdot\left[(\vec{\omega}+\vec{f})\cdot\nabla\vec{v}\right] + \nabla\theta\cdot\nabla\times\vec{F} \tag{18}$$

Noting that $\frac{d(\ )}{dt} = \frac{\partial(\ )}{\partial t} + \vec{v}\cdot\nabla(\ )$, it can be shown by this simple expansion,

$$(\vec{\omega}+\vec{f})\cdot\frac{d}{dt}\nabla\theta = \left[(\vec{\omega}+\vec{f})\cdot\nabla\right]\frac{d\theta}{dt} - \nabla\theta\cdot\left[(\vec{\omega}+\vec{f})\cdot\nabla\vec{v}\right] \tag{19}$$

Combining (18) and (19), and noting that the baroclinic term in

(18) vanishes since Θ is only a function of pressure and density, we obtain

$$\frac{d}{dt}\left[\frac{(\vec{\omega}+\vec{f})\cdot\nabla\theta}{\rho}\right]=\frac{1}{\rho}\left[(\vec{\omega}+\vec{f})\cdot\nabla\right]\frac{d\theta}{dt}+\frac{1}{\rho}\nabla\theta\cdot\nabla\times\vec{F} \qquad (20)$$

The quantity in brackets on the left-hand side is the potential vorticity. For frictionless, adiabatic flow, this becomes a conservation theorem; stating that as $\nabla\Theta$ is decreased (the isentropes are spread apart), vorticity is produced by a stretching of the air columns between the potential temperature surfaces.

By taking the component of absolute vorticity in the direction of the Θ -gradient, equation (20) becomes

$$\frac{d}{dt}\left[\frac{(\zeta_\theta+f_\theta)|\nabla\theta|}{\rho}\right]=\frac{1}{\rho}\left[(\zeta_\theta+f_\theta)\left|\nabla\frac{d\theta}{dt}\right|\right]+\frac{1}{\rho}|\nabla\theta|F_n \qquad (21)$$

where F_n is the component of frictional torque in the direction of $\nabla\Theta$. Since Θ changes most rapidly in the vertical, this part of $\nabla\Theta$ will dominate, and we obtain (using the hydrostatic approximation)

$$\frac{d}{dt}\left[-g(\zeta_\theta+f_\theta)\frac{\partial\theta}{\partial p}\right]=\frac{1}{\rho}(\zeta_\theta+f_\theta)\left|\nabla\frac{d\theta}{dt}\right|-g\frac{\partial\theta}{\partial p}F_n \qquad (22)$$

In our case study adiabatic flow will be assumed, so the conservation of potential vorticity, P, may be used with (4) and (10) to improve the accuracy of the trajectory.

The terms comprising the potential vorticity now will be discussed. The $\frac{\partial \theta}{\partial p}$ term is a measure of the stability of an air parcel that is subjected to vertical displacement, and it is always negative. In this thesis it is evaluated by a centered finite-difference approximation using a θ -interval of four degrees Kelvin:

$$\frac{\theta_{i+4} - \theta_{i-4}}{\Delta p} \tag{23}$$

The other term in P is the absolute vorticity, $(\zeta_\theta + f_\theta)$, on an isentropic surface. The difference between f and f_θ (the vertical component of the earth's rotation on an isentropic level) is on the order of 10^{-6} sec^{-1} on the more steeply sloped isentropes, so f will be used in place of f_θ throughout this study. The relative vorticity, ζ_θ , is computed from the pattern of wind flow on the θ- surface,

$$\zeta_\theta = \frac{\partial v}{\partial s_\theta} + \frac{v}{r_\theta} \tag{24}$$

where v is the wind speed and r_θ is the radius of curvature of the streamlines. The shear term, $\frac{\partial v}{\partial s_\theta}$, is evaluated in units of sec^{-1} by means of a finite-difference technique similar to (23) (using 120 nautical miles as the distance increment almost everywhere). The curvature term, $\frac{v}{r_\theta}$, is evaluated as $v \frac{\partial \phi}{\partial s_\theta}$; where s_θ is parallel to the streamlines and ϕ is the wind direction in radians. Using 120 nautical miles for the distance increment, this term is also evaluated by finite-difference methods. It must be noted that

errors in the computation of β_θ will result, since the transmitted wind data has been rounded off to the nearest ten degrees. One should also realize that the vorticity on an isentropic surface is different than on an isobaric surface. The difference occurs principally in the wind shear term, and it is a result of the steeper slope of the θ surface. In some cases its possible to have cyclonic shear on one of the surfaces and anticyclonic shear on the other.

In the computation of potential vorticity for this case study, it became apparent that the stability term was the most important in determining the size of P. Simply on this basis, high values of P must be found in the stratosphere, and in fact they can exceed those in the troposphere by one or more orders of magnitude. If we consider the case of non-adiabatic, frictionless flow, the vertical variation of heating is the most important term contributing to a change of P in equation (22).

$$\frac{dP}{dt} = -g(\beta_\theta + f)\frac{\partial}{\partial p}\left(\frac{d\theta}{dt}\right) \qquad (25)$$

Thus, over a sufficient time period, heating above a region and cooling below it will increase P. In the stratosphere the "heating above" part occurs in the ozone layer and the "cooling below" part occurs in the upper troposphere. Hence, the stratosphere will have high values of potential vorticity. In tropospheric regions far enough from the ground and far enough from condensation processes, $\frac{d\theta}{dt}$ is a small quantity and P is approximately conserved. Thus, it is reasonable to attribute stratospheric origin to air parcels in

the dry, middle-tropospheric fronts if they have high values of potential vorticity.

In the next two sections the particular front found in February 1964 will be described, and its evolution in time and space will be examined. Then in the following section the kinematic relation (4), the energy relation (10), and conservation of potential vorticity will be used to develop air parcel trajectories. Finally, as a direct result of the trajectories, the important frontogenetical processes occurring in this case will be explored.

III. SYNOPTIC SITUATION: 18-20 February 1964

In attempting to verify the existence of a high-tropospheric front, it was necessary to sift through weather maps at the 500-mb level. A particularly intense temperature gradient was found to exist along the southeastern coast of the United States on 20 February 1964 at 0000 GMT. Noting that this gradient at 500 mb implied a strong high-tropospheric front, the author decided to look back in time to see if its origin could be determined. In anticipation of the existence of the front at higher levels at earlier times, as Sanders had found in several cases, the author decided to observe the events starting on 18 February at 1200 GMT. By using methods to be explained in later sections, a distinct frontal zone could be easily observed only on 20 February (0000 GMT), while vague frontal areas seemed to exist twelve hours earlier.

At 1200 GMT on 18 February a rather weak trough was located aloft over the central United States and a small surface wave was appearing on the Florida-Gulf coast. Cold air was beginning to filter out of Canada over Minnesota, and cold advection through the disturbance aloft implied a rapid deepening. In twenty-four hours the surface storm center had deepened from 1000-mb to 984-mb and was located off the southeast New Jersey coast (figure 1). Aloft, a pinwheel shaped height contour appeared over the northern Mid-West and seemed to show two separate disturbances (figure 2). The eastern prong was associated with the intense surface storm, whereas the

southern prong (over Arkansas) was not associated with any organized surface system, although light precipitation was falling to the east. By now a rather intense temperature gradient was associated with this latter portion of the trough. Just an observation of the wind field shows that a great deal of kinetic energy has been put into the system, as wind speeds in excess of one hundred knots were observed over the Southeast. Methods employed in the next section will show the front was not very distinct.

On the twentieth at 0000 GMT the upper-level front has greatly intensified. The 500-mb trough has deepened a bit (figure 3), and the temperature gradient has increased, being about twenty degrees Celsius in 230 nautical miles (line AB); yet the surface storm has had no decrease in central pressure and has shown little horizontal movement (figure 4). The fact that the high-level front has intensified long after the surface front (now over Cuba) gives us a hint that there is little or no connection between the two. The cloudiness that is noted in the surface observations below the high-level front is in no way a reflection of the moisture associated with it. These are low level strato-cumulus clouds formed by daytime heating in an unstable air mass.

IV. METHODS OF LOCATING THE FRONT

A. Plotting Radiosonde Data

Now that the general features of the frontal situation have been discussed, radiosonde data must be plotted for the four time periods[1] so that the baroclinic zone can be located in the vertical. A feature of these intense mid-tropospheric fronts (other than the marked temperature gradient) is the occurrence of strong vertical wind shear. The large, dry temperature inversions determining the vertical extent of the front are seen over Tampa and Jacksonville on the twentieth (figures 5 and 6). An eighteen knot wind shear between 9000 feet and 10,000 feet at Tampa is coupled with the increase of eight degrees Celsius above 700 mb. Similarly a fifty knot wind shear between 12,000 feet and 14,000 feet at Jacksonville is tied with the strong temperature inversion at 600 mb. This coupling of temperature and wind is simply a result of the thermal wind relationship.

If we observe the change in direction of the air flow at both stations, we see a backing of the wind with height, which implies cold advection through the pertinent layer and therefore descending motion. However, this is on the eastern side of the trough where vorticity advection would imply ascending motion. Thus we cannot

---

1. 18 February, 1200 GMT; 19 February, 0000 GMT and 1200 GMT; 20 February, 0000 GMT.

infer the vertical motions from the wind profile, but since the air parcels are relatively warmer than their surroundings, we can say that they have been descending during a large portion of their journey.

An inherent problem in using transmitted radiosonde data has been the loss of some information from the original record. Wind directions are rounded off to the nearest ten degrees and significant points on the soundings are determined by the observer. The reprocessing of raw data might be advisable for a detailed study[1], but we are observing a strong feature that will be discernible despite errors in the data. Also, since we are concerned with large variations in space and in time, a detailed analysis simply is not feasible.

Now that one has determined the importance of vertical wind shear in locating the baroclinic zone, the radiosonde data for the region where the front exists (found by inspecting the thermal field at 500 mb) then is sorted to find these strong vertical shears (twenty knots in two thousand feet is arbitrarily chosen as a critical value). The pertinent stations are plotted on pseudo-adiabatic charts, along with a ring of stations surrounding the region of probable frontal activity. In trying to determine the number of pseudo-adiabats to analyze, it is wise to choose more than are initially necessary, since most of the radiosonde network will be needed eventually.

---

1. Danielsen (1960) has performed just such a study and has found many stable layers on the order of 1000 feet in depth.

B. Potential Temperature Analyses

In regions of adiabatic flow, we have seen (II,A) that the First Law of Thermodynamics can be expressed as the conservation of potential temperature following an air parcel. Since we are discussing an extremely dry region, the above statement of the First Law can be used to trace air particles. This is a good reason for using potential temperature as a dependent variable.

Now that all the radiosonde data has been plotted up (IV,A), the front will be located on quasi-horizontal pressure levels by means of isentropic surfaces. The reason for analyzing the potential temperature surfaces is to locate the front more accurately in the horizontal by using the information that we have in the vertical. If we had used the actual temperature gradient in locating the front, about all we could hope to see between stations would be a uniform change in temperature (as along AB - figure 3). By using the isentropic analyses, we have employed the stability values at the various stations to give us a more accurate location of the front and a more realistic picture of its intensity (compare figures 3 and 10).

A discussion of the development of the isentropic analyses follows. Since our front is probably located somewhere between 300 mb and 700 mb, the highest and lowest potential temperatures at these pressures, respectively, are determined from the pseudo-adiabatic charts. In order to visualize what is happening in the vertical, isentropic surfaces plotted at every $4^{\circ}K$ from the lower

limiting value are sufficient. On each such level for every station, the pressure and the mixing ratio for this particular potential temperature are plotted, along with the difference in pressure between this Θ-surface and the one above. For each of these isentropic levels the pressure is analyzed in fifty-millibar intervals with the aid of the difference field of the lower level. A map of the pressure on a Θ-surface is now obtained, and it is quite trivial to plot the Θ-field at a specific pressure level. This results in a map of the thermal field at each isobaric surface. Levels 300 through 700 have been chosen in this study. A spot check on the analyses may be made by using the following relation:

$$\frac{\partial \Theta}{\partial x} = -\frac{\partial \Theta}{\partial p}\left(\frac{dp}{dx}\right)_{\Theta} \qquad (26)$$

The term on the left is evaluated on an isobaric surface and the last term on the right is evaluated on an isentropic surface. Finite difference methods are used, where $-\frac{\partial \Theta}{\partial p}\left(\frac{dp}{dx}\right)_{\Theta} = -\frac{\Delta\Theta}{\Delta p}\frac{(\Delta p)_{\Theta}}{(\Delta x)_{\Theta}}$. $\Delta\Theta$ is set equal to eight degrees Kelvin, and noting that $(\Delta p)_{\Theta}$ and Δp are different, the terms on the right side of (26) are evaluated at the middle point of the distance increment $(\Delta x)_{\Theta}$. Equation (26) should be satisfied if the analyses are correct.

The temperature analyses on the isobaric surfaces for 18 February, 1200 GMT and 19 February, 0000 GMT have not been presented since the thermal fields do not show any definite frontal zones. In several places two potential temperature lines came close together

for a little distance, but two isentropes do not constitute a strong front. On the nineteenth at 1200 GMT, the vigorous zone has not yet appeared; however, a bunching of the θ -lines is evident over Arkansas and Louisiana (figures 7 and 8). The thermal fields for 400 mb and 500 mb have been included mainly as a comparison for these fields twelve hours later.

On 20 February at 0000 GMT, the baroclinic zone has intensified immensely and is located on the southeast side of the trough at 500 mb. The θ -fields for pressures from 400 mb to 700 mb have been included (figures 9, 10, 11, and 12). The first thing to notice is how the intensity has developed in such a short time. At 1200 GMT on the nineteenth the maximum gradient to be found at 500 mb is approximately thirteen degrees Kelvin in seventy nautical miles over a small region in eastern Texas. At 0000 GMT on the twentieth, the maximum gradient has become sixteen degrees Kelvin in seventy nautical miles over a much bigger region. This gradient has been verified using (26); and the zone has become much longer, thereby implying that some strong frontogenetical process has occurred in this short time. By looking at each pressure analysis, one may see that the cold air boundary to the frontal zone is probably the 303°K isentrope at 400 mb, and it is the 295°K isentrope at the lower surfaces. Similarly the warm air boundary changes as each pressure level is observed—being θ = 315°K, 311°K, 307°K, 303°K, respectively, at the four pressure levels starting at 400 mb. Thus there appears to be a shift towards higher isentropes at higher elevations.

The study of the frontal life cycle can no longer be continued, for it now moves out over the Atlantic Ocean where data is sparse. However, a quick check at 1200 GMT on the twentieth reveals a remnant of the front at 800 mb over Miami and Key West. Comments concerning the frontogenetical processes and the origin of air parcels composing the zone are deferred to a later section.

C. Potential Temperature Cross Section Analyses

Since the front has been located quasi-horizontally, it is desirable to see what it looks like in the vertical. Vertical cross-sections using potential temperature are perhaps the best. Actual temperature cross-sections become very complicated, whereas the potential temperature cross-sections are relatively smooth. Both the thermal wind relation and the isentropic analyses (IV,B) have been utilized in the construction of vertical cross-sections perpendicular to the direction of air flow (analyzed for every two degrees Kelvin). As expected nothing striking was found in those analyzed for 18 February at 1200 GMT; however, on the nineteenth at 0000 GMT several stable zones were found over Texas between the 293°K and 299°K isentropes (figures 13 and 14). Since these potential temperatures are clearly the same as those found on the cold side of the baroclinic zone twenty-four hours later, it seems that the smaller temperature interval used has exposed possible beginnings of the front. If this is the case, then the frontal zones certainly are travelling more slowly than the air parcels that are flowing through them. If the location of these zones is arbitrarily

taken as central Texas, then they are moving at approximately forty knots, whereas the air parcels are moving through them at speeds often over one hundred knots. Since only the 295°K and 299°K isentropes are found in these zones, it is easy to show how the "front" was missed in the isentropic analyses (IV,B).

On the nineteenth at 1200 GMT several relatively strong zones have been found in the cross-sections. At 500 mb between Corpus Christi and Lake Charles an intense front is observed from the 303°K isentrope (figure 15). We note that these potential temperatures are higher than those composing the front twelve hours later. This zone may eventually dissipate, but it seems more reasonable to associate it with the higher portions of the intense front on the twentieth. Further east on the nineteenth a less intense frontal zone is found between Tampa and Montgomery at 700 mb between the 291°K and 301°K surfaces (figure 16).

On the twentieth, the strong baroclinic zone observed on the isentropic charts is displayed in a vertical cross-section (figure 17-18).[1] The isotach pattern (figure 19) and the moisture pattern (figure 20) have been included. There are several significant features of these analyses. First, the frontal zone is actually a combination of two potential temperature groupings. As noted in section (IV,B), between 700 mb and 500 mb, the 295°K and 311°K isentropes bound the zone. Above 500 mb, the baroclinic zone shifts to

---

1. Figure 18 is analyzed for every 4°K so that the essential features of the front can be presented in a clear manner.

higher isentropes (around θ = 315°K) until it reaches into the stratosphere near 300 mb. The fact that a portion of the front extends into the stratosphere will be important in relating the tropopause boundary to the frontal boundary in a later section. We note how the frontal isentropes curl upward over Key West and spread apart to the south, which seems to be more of an indication that this front is not an extension from the surface. A second feature of this situation is the location of the front at 500 mb. This is near Charleston and is vertically under the jet stream, a fact discussed earlier by Palmen (1948). The final point to be made concerns the moisture analysis. The extremely dry air that constitutes the front is vividly shown over Tampa and Jacksonville. Moisture streaming in aloft over the very dry layer at Tampa implies that the flow at these higher levels is probably coming from a more southerly and more moist region.

In this section various methods have been used to analyze the intense middle-tropospheric front. It has been shown by an examination of the attached diagrams that this baroclinic zone is rather diffuse until it reaches the southeastern side of the trough. Many and varied stable layers exist prior to the twentieth on the western side of the trough. Of course, a fairly strong zone is found north of Corpus Christi on the nineteenth, and it may extend over the Gulf of Mexico; but these isentropes are of different values from those on the twentieth and therefore may not be part of the frontal zone. Using the methods of analysis of the previous section, we

have further shown that the baroclinic region is characterized by a large horizontal temperature gradient and an associated strong vertical wind shear. This region is very stable and very dry which may suggest descent from higher elevations. It is this last point that must be verified by a trajectory analysis using the methods of section II.

V. DISCUSSION OF RESULTS

A. Trajectories

In order to make a systematic study of one of these high-level frontal zones, specific isentropic surfaces must be chosen. An examination of the potential temperature cross-section for 20 February at 0000 GMT (figure 18) reveals that the 295°K, 303°K and 311°K isentropes are the approximate boundaries and mid-point of the front (especially south of GSO). By using (3), the ψ-field for these three surfaces was computed at 1200 GMT on the nineteenth and at 0000 GMT on the twentieth, and the winds at these levels were determined by a linear interpolation of the transmitted teletype data. The end points of the trajectories were chosen in the frontal zone for 20 February (0000 GMT) and are labelled on the isotherm fields of the 500, 600 and 700-millibar surfaces (figures 10-12). Other than aligning the points perpendicular to the front for each isentrope, the choice of positions was completely arbitrary.

Isentropic trajectories using (4) and (10) were then constructed (figures 21-29). In all cases it was found that simply using (4) did not suffice, for the initial points of these trajectories had to be moved to the south and west in order to satisfy (10). In most cases the air parcels remained on the cyclonic side of the jet; however, those trajectories ending at 500 mb on the 311°K surface were found to have come from the anticyclonic side. There is no possible way to keep these trajectories on the cyclonic side of the jet without

violating either (4) or (10). These five particle paths imply that a substantial increase in absolute vorticity occurs, and this will make it difficult to conserve potential vorticity (see V, B).

The initial and final pressures given on the trajectory diagrams show that in all cases there is descent. The 311°K isentrope represents the warm air side of the frontal zone at 500 mb and the 303°K isentrope represents this same side at 600 mb and 700 mb. For the three pressure levels the 295°K isentrope is the cold air boundary of the frontal zone. At 500 mb and 700 mb an indirect thermal circulation is clearly visible; thus confirming an observation by Reed (1955). At 600 mb there appears to be a direct thermal circulation for the two trajectories presented (figures 23,24); however, a similar analysis, which has not been included, shows a slight indirect circulation for trajectories ending over southern Alabama (at this same level).

In order to see if the trajectories were reasonable, several of them were studied in conjunction with radiosonde data. The trajectory ending at point B near TPA at 700 mb on the 303°K surface is observed to start at 549 mb near CRP on the nineteenth (figure 22). The 303°K surface which is found in the middle of an intense front over TPA (figure 5) is observed to be in the middle of a weaker front ober CRP (figure 30). Thus the front existed on the nineteenth, even though it may have been difficult to observe it at these isentropes in the isotherm field (figure 7,8).

B. Conservation of Potential Vorticity

A good way of assessing the validity of the trajectories is to look at the potential vorticity of the initial and final points. In the case of adiabatic flow, the conservation of P implies that as the absolute vorticity on an isentropic surface increases (decreases), the stability of the air parcel must decrease (increase). The potential vorticity of the initial and final points of the trajectories are presented in appendix II. In almost all cases potential vorticity is increasing. There is some negative change of P on the western end of the front at θ = 303°K, and this is borne out by the trajectory ending over southern Alabama on this isentropic surface. Staley (1960) found large positive potential vorticity changes in the upper troposphere on the cold side of a front and large negative changes in the frontal zone and around the southern periphery. In our case positive changes of P occur throughout the baroclinic zone.

On the 295°K isentropic surface potential vorticity is conserved quite well along most of the trajectories, and the absolute vorticity and stability change in the required senses. However, conservation of P becomes more difficult on the two higher surfaces. At the 303°K level, the trajectory ending at D is particularly non-conserving. The absolute vorticity has increased slightly, but the stability has increased tremendously. By shortening the trajectory about 250 nautical miles we might conserve P, but then (4) would be violated. Thus some non-adiabatic or frictional effect must be occurring.

On the 311°K surface there is a huge discrepancy between initial and final values of P. In all these cases the vorticity has increased because the parcels started on the anticyclonic side of the jet and ended on the cyclonic side. At the same time stability values have become much larger. The potential vorticity on the 311°K surface (figures 31, 32) has increased markedly in twelve hours over the eastern United States, especially over the southern Appalachains. P-values consistent with those of the later time may be found on the nineteenth; however, those values in the 70's and 80's on the twentieth certainly are not represented at the earlier time. A diagram has been included to show the inability to conserve potential vorticity, energy (10), and kinematics (4) simultaneously (figure 33). The trajectory on the 311°K surface represented by line MN is the one determined by using (4) and (10), while the dotted line determines the location of a potential vorticity value that agrees with the final value. The line ON depicts a trajectory which will conserve P and energy, but will not satisfy (4). The average velocity along MN is 100 knots and the average velocity along ON is 60 knots, clearly implying the existence of some diabatic or frictional effect.

Conservation of P is a more stringent requirement than the energy equation (10), since $\frac{\partial}{\partial p}\left(\frac{d\theta}{dt}\right)$ and F_n must be zero (see (22)) for the former to hold, whereas only $\frac{d\theta}{dt}$ and friction must be zero for the latter to be valid. There are three possible reasons for non-conservation of potential vorticity. First, air parcels can be moving adiabatically on a particular surface, but diabatic motions

may exist on adjacent surfaces. In this case the isentropic trajectory is correct, but diabatic effects cause the potential vorticity of a parcel to change. Second, the flow may be adiabatic, but the frictional components normal to the isentropic surfaces (F_n) may not be zero. Again the trajectories we have constructed are correct, but P is not conserved. Finally, we may simply infer that the flow is non-adiabatic, the trajectories are wrong, and P probably will not be conserved.

We note that the diabatic effects have a direct bearing only on stability changes, whereas the frictional effects influence only the relative vorticity. For the five trajectories on the 311°K surface, the movement from the anticyclonic to the cyclonic side of the jet causes the relative vorticity to increase from very small negative values to large positive ones. At the same time the stability greatly increases, so naturally P is not conserved. Throughout most of the lengths of the trajectories the relative vorticity is positive and changing in the positive sense; so if friction is thought of as a dissipative mechanism, such increases would be opposed by these frictional torques. Since the relative vorticity increases by necessity, friction appears to play a small role in changing P. Alternatively, if the change in stability is a result of the motion field, then S_θ would necessarily decrease. This does not happen. If we use the above two arguments, diabatic effects seem to be more important in changing P than friction on the 311°K surface.

For two trajectories (D,G) on the 303°K surface, along which there is a strong increase in P, the relative vorticity is positive and changes slightly in the positive sense, while the stability grows immensely (from .12 to .47°K $(mb)^{-1}$ along D; from .26 to .41°K $(mb)^{-1}$ along G). The main cause of the increase in P is found to be the stability change, thus implying that diabatic effects might be important. If the stability increase is a result of the motion field, then this effect plus friction will cause a decrease in vorticity along the particle path. Since the vorticity increases, it seems that diabatic influences are also the major causes of changes in P on the 303°K surface.

Recalling that low clouds exist below the frontal region, we note that the resultant radiational cooling near their tops can provide a positive diabatic contribution to the potential vorticity changes. By using equation (25) we attempt to attribute all of the potential vorticity changes to diabatic effects. Taking the largest change in P (about 40 units) and using the associated absolute vorticity we can solve for $\frac{\partial}{\partial p}\left(\frac{d\theta}{dt}\right)$ and get a cooling rate on the order of 10°C per day (per thousand feet). Moller (1951) notes possible cooling rates on the order of 2°C to 5°C per day above clouds, thus making our computed value quite high; however, diabatic effects of this magnitude can exist in most of our cases, if we observe the average change in P is less than 20 units.

Of course these cooling rates apply close to the cloud tops, and an examination of the radiosonde data for the twentieth reveals that

the cloudiness is probably several thousand feet below the frontal zone. However, if such cooling rates are assumed to exist, diffusion and turbulent mixing will extend such radiational effects upward-affecting the 295°K surface more strongly than the higher isentropes. This relative cooling of the cold air boundary intensifies the temperature gradient and thus helps to cause frontogenesis. This diabatic effect also means that air parcels have descended from higher levels than simple adiabatic trajectories show, possibly making observed indirect circulations less intense (and direct circulations more intense).

From this discussion we can see that the isentropic trajectories may be in error. However, since the strength of the diabatic effects can never be known, we shall assume that the non-conservation of P (and all its attendant problems) will not prevent us from obtaining reasonable qualitative results on the three potential temperature surfaces. Although several trajectories were altered slightly in an attempt to conserve P (if (4) was not violated by very much), the majority were left as they were before the potential vorticity analysis was started.

C. Stratospheric Origin of Trajectories

Since several of the air parcels have come from levels above 400 mb and have high P-values, it is suspected that they have descended from the stratosphere. The exact location of the tropopause is unknown, so the identification of air parcels with the stratosphere

may be difficult. From the vertical cross-sections it is apparent that many shallow stable layers exist in the high troposphere, each of which might be mistaken for the tropopause. These layers are of differing phase and amplitude and may be far apart at one station and close together at the next; causing the conventional tropopause to oscillate in the cross-section. Difficult as it may seem to label the origins of air parcels by using the reported tropopause, we assume that high potential vorticity values will signify stratospheric air. As an example of the problem of defining the actual tropopause, the intersection of the reported tropopause on the 311°K surface for the nineteenth is compared with the potential vorticity values at this isentropic level (see figures 31 and 34). P-values exceeding 20 or 25 are definitely stratospheric, yet Jackson, Mississippi with a potential vorticity over 60 (at 394 mb) on the 311°K surface reports the conventional tropopause at 100 mb.

As a first approximation in determining the origin of the frontal air parcels we can simply compare the initial points with the reported tropopause. Using this method, only air parcels ending at points E, F, G on the 295°K and 303°K surfaces and the one ending at point H on the 303°K surface (all at 500 mb) are initially found above the reported tropopause. If this were the only means of identifying air parcels, all the others would have a tropospheric origin, unless they had been in the stratosphere at an earlier time.

As a second approximation in determining the origins of parcels, we observe their potential vorticity values. A study of the reported

tropopause on the twentieth reveals that none of the final points of the trajectories are above this boundary, so that high P-values at the end points will imply a stratospheric origin. In addition to the trajectories noted above, this method shows that parcels reaching points D and I on the 303°K surface and points G, H and I on the 311°K surface have a stratospheric beginning.

It is interesting to note a potential vorticity maximum in the middle of the front ($\ominus$ = 303°K) at points E, F and G (appendix II). Although this is a partial result of higher stability on the 303°K surface, it does suggest a tongue-like extrusion of stratospheric air that has been noted by many authors (Reed, 1955; Danielsen, 1964). However, it is difficult to simply say that the tropopause has subsided to a low elevation and become a frontal boundary. This does not explain the existence of the upper frontal boundary, above which the air is tropospheric. Danielson (1964) and others have postulated that the tropopause has become folded and a wedge of stratosphere air has slipped into the troposphere. Danielsen further explains how this folding can result from a suitable combination of geostrophic winds and vertical velocities near the tropopause. In anticipation of seeing this tongue of stratospheric air, potential vorticity and absolute vorticity values have been analyzed on the vertical cross-section for the twentieth at 0000 GMT (figures 35, 36). We will not see the stratosphere extending down into the front, since we have values at only three isentropic levels, but an extruded appearance is clearly visible. The sharp change in the

P-values outlines the frontal boundaries in the lower and middle troposphere. Especially high values of potential and absolute vorticities are noted between 400 mb and 500 mb. It seems that stratospheric air can be identified almost down to 700 mb in the frontal zone near Tampa, then the front becomes associated with a stable layer in the tropical air over southern Florida (see Figure 18).

D. Frontogenesis in the Thermal Field

While we have attempted to discuss the front in the middle troposphere on the basis of isentropic trajectories, it becomes necessary to determine the various mechanisms at work. According to Miller (1948), the intensity of frontogenesis in the horizontal may be expressed as,

$$-\frac{d}{dt}\left(\frac{\partial\theta}{\partial y}\right)=-\frac{\partial}{\partial y}\left(\frac{d\theta}{dt}\right)+\frac{\partial\omega}{\partial y}\frac{\partial\theta}{\partial p}+\frac{\partial v}{\partial y}\frac{\partial\theta}{\partial y} \qquad (27)$$

where the y-axis is directed toward the cold air, parallel to the temperature gradient. The left side of (27) will be positive for frontogenesis. The first term on the right is the effect of diabatic heating and cooling, and will be frontogenetical if there is more intense heating in the warmer air than in the colder air. The positive effect of this term has been noted (V, B) in relation to radiational cooling at the tops of clouds. However, since we have assumed the flow to be adiabatic and since any diabatic effects are

impossible to measure, this term shall be neglected. The second term on the right is the tilting effect, and it expresses the influence of vertical motion. The third term on the right is the confluence term, and it represents intensification due to the horizontal wind field. In our case the size of this final term is very sensitive to the wind analyses, since strong winds are blowing nearly parallel to the frontal zone.

The effects of the various terms were observed at the mid-points of the trajectories ending in the middle of the frontal zone. For those ending at E, F and G, the trajectory chosen was along the 303°K surface; however, for the other trajectories, intermediate paths were interpolated between those along the flanking isentropic surfaces. The vertical velocity was determined from the initial and final pressures over the twelve hour period. The stability at the mid-points was computed as a simple average of the values at these points for the two time periods. Since the y-axis must be perpendicular to the isotherms, an intermediate temperature field was constructed at the appropriate pressure level by averaging the initial and final patterns. This field was corrected by using several radiosonde stations that reported at 1800 GMT on the nineteenth. Values of $\frac{\partial v}{\partial y}$ were obtained from the wind field at 1800 GMT for the trajectories ending at E, F, G, H and I; but an average of the initial and final values of this confluence term was used for the other trajectories, since their mid-points were close to or over the Gulf of Mexico. The $\frac{\partial \theta}{\partial y}$ term had to be evaluated

by averaging the initial and final values of the temperature gradient. The values of the various terms were then calculated as twelve hour averages. It must be noted, before the computations are started, that this analysis is quite susceptible to error, since it depends upon the positioning of the trajectory mid-points.

The values of the various terms for six of the trajectories are included in table I. The computations for the other three (A, B and D) were extremely poor, probably due to the lack of data over the Gulf of Mexico.

Table I

Final points	C	E	F	G	H	I
Tilting effect	-4.3	+4.1	+4.8	+5.0	+3.1	+0.7
Confluence effect	+7.6	-0.7	+5.2	+2.6	+6.2	+7.6
Total (computed)	+3.3	+3.4	+10.0	+7.6	+8.3	+8.3
Total (observed)	+2.1	+3.8	+8.2	+6.3	+9.7	+8.0

The importance of the confluence effect for point C is certainly necessary to overbalance the frontolytical effect of direct circulation. The fairly close agreement between the observed intensification and the computed intensification lends support to our entire analysis, even though problems arose for the three trajectories noted above.

The mid-points of the trajectories ending at H and I at 500 mb appear to be in the frontal zone, whereas the mid-points of E, F, G seem to be near the entrance of the baroclinic zone. From this we might surmise that the tilting term is relatively important in the entrance region and the confluence term predominates in the frontal

zone itself. The mid-point of trajectory C is probably near the entrance to the front, but the strong confluence term is necessary due to the direct circulation at 800 mb. For the two trajectories ending at 700 mb (not listed), the tilting effect was so strong that the computed intensification was an order of magnitude larger than the observed intensification.

The dynamical aspects of frontogenesis have been discussed, and the rapid development of our front on the southeast side of the trough now can be studied. In an attempt to uncover the reason for the strong growth of the front, the 500-mb charts and the 650-mb vertical velocity maps were examined for the period, 18-20 February. Other than noting the existence of a vigorous trough in the Pacific Northwest that moves down into Utah on the twentieth, the general synoptic situations have been discussed in section III.

The first term to be examined is the effect of horizontal confluence. It is evident that any trajectory ending in a hypothetical front over Texas (using 500-mb data for the first two time periods) will be passing through a diffluent region caused by the trough in British Columbia (figure 37). It is only when the major trough in the East is far enough from the disturbance in the West (on the nineteenth at 1200 GMT and especially on the twentieth at 0000 GMT) that strong confluent flow can exist on its southwest side (figures 2,3).

The directions and perhaps the magnitudes of vertical velocities at higher levels can be inferred from those at 650 mb, and thus we may observe the effect of the tilting term. In all cases the descent

is stronger to the south, therefore giving us confidence in the indirect circulations that we obtained in most cases by using the trajectory analyses. In the first two time periods, trajectories from this hypothetical front over Texas probably will be rising initially and then descending. In such a case the tilting term may be reduced. For the last time period, we are far enough from the western trough that there is descent throughout the particle paths. Also, a small region of very strong descent exists over southern Louisiana on the twentieth, thereby implying good indirect circulation if the southernmost of a pair of trajectories passes through it.

VI. CONCLUSIONS

An upper-tropospheric frontal zone has been examined over the southern and central portions of the United States for 18-20 February 1964. Very diffuse frontal zones appear over Texas on the nineteenth at 1200 GMT to the southwest of the 500-mb trough. Air parcels passing rapidly through this region are being subjected to frontogenetical and frontolytical processes. Rapid frontogenesis occurs on the southeast side of the trough (20 February at 0000 GMT) only when the trough in the west is distant enough to allow the various dynamical mechanisms to work in a strong positive sense and increase the frontal intensity. The front, which exists over the southeast, extends from above 400 mb to below 700 mb and its boundaries are shifted towards higher isentropes at higher elevations. The rapid intensification does not appear to be coincident with any surface deepening, although the 500-mb trough strengthens slightly. The baroclinic zone seems to be connected to a stable layer in the tropical air, but does not appear to be attached to the surface cold front. The zone is characterized by a strong vertical wind shear, a strong temperature gradient and a high stability; and it is located vertically below the jet core at 500 mb.

Very dry conditions and height above the ground gives one confidence in using the adiabatic assumption to analyze the front. Three-dimensional isentropic trajectories, terminating in and near the intense portion of the frontal zone, were constructed using the

energy equation and potential vorticity as guides. Contrary to Staley's result in 1960, potential vorticity was observed to increase through most of the frontal zone. The change in P has been attributed mainly to diabatic effects, but it is assumed that this non-conservation will not seriously impair our adiabatic trajectories. Descending air exists throughout the region, and indirect circulation is found everywhere except for those air parcels ending at 600 mb. The descent exists on both sides of the jet, and in several cases it seems that parcels cross the jet before descending. Evidence based on the trajectory analysis and P-analysis shows the existence of stratospheric air in the frontal zone. The cross section prepared for the twentieth displays the tongue-like extrusion of stratospheric air that has been noted by several authors.

The frontogenetical processes at work in this case are both the horizontal confluence and vertical tilting effects. This is contrary to the results of Reed and Sanders (1953) where the tilting effect predominated. From a quick look at the trajectories it appears that the tilting term is relatively important at the entrance to the front, whereas the confluence term is important in the frontal zone itself.

APPENDICES

APPENDIX I

The following table presents the values of a distance increment, 2Δ, for various latitudes. It is used if the contours of are analyzed at intervals of 600 m^2/sec^2. The number (and fraction) of contour intervals contained in 2Δ is multiplied by 10 to give the geostrophic velocity in m/sec.

Latitude (degrees)	2Δ (degrees of latitude)
25	8.8
30	7.4
35	6.5
40	5.8
45	5.2
50	4.8
55	4.5

APPENDIX II

	Θ = 295°K		Θ = 303°K		Θ = 311°K	
	P_i	P_f	P_i	P_f	P_i	P_f
A	4	8	20	29		
B	4	7	19	19		
C	9	12	11	20		
D	11	16	10	44		
E	26	24	33	30	4	16
F	26	28	41	43	5	19
G	22	31	30	63	6	25
H			36	44	8	40
I			29	29	15	54

P_i is the initial value and P_f is the final value. The units of P are $\frac{^oK}{mb}\frac{cm}{sec^3} \times 10^{-3}$.

FIGURES

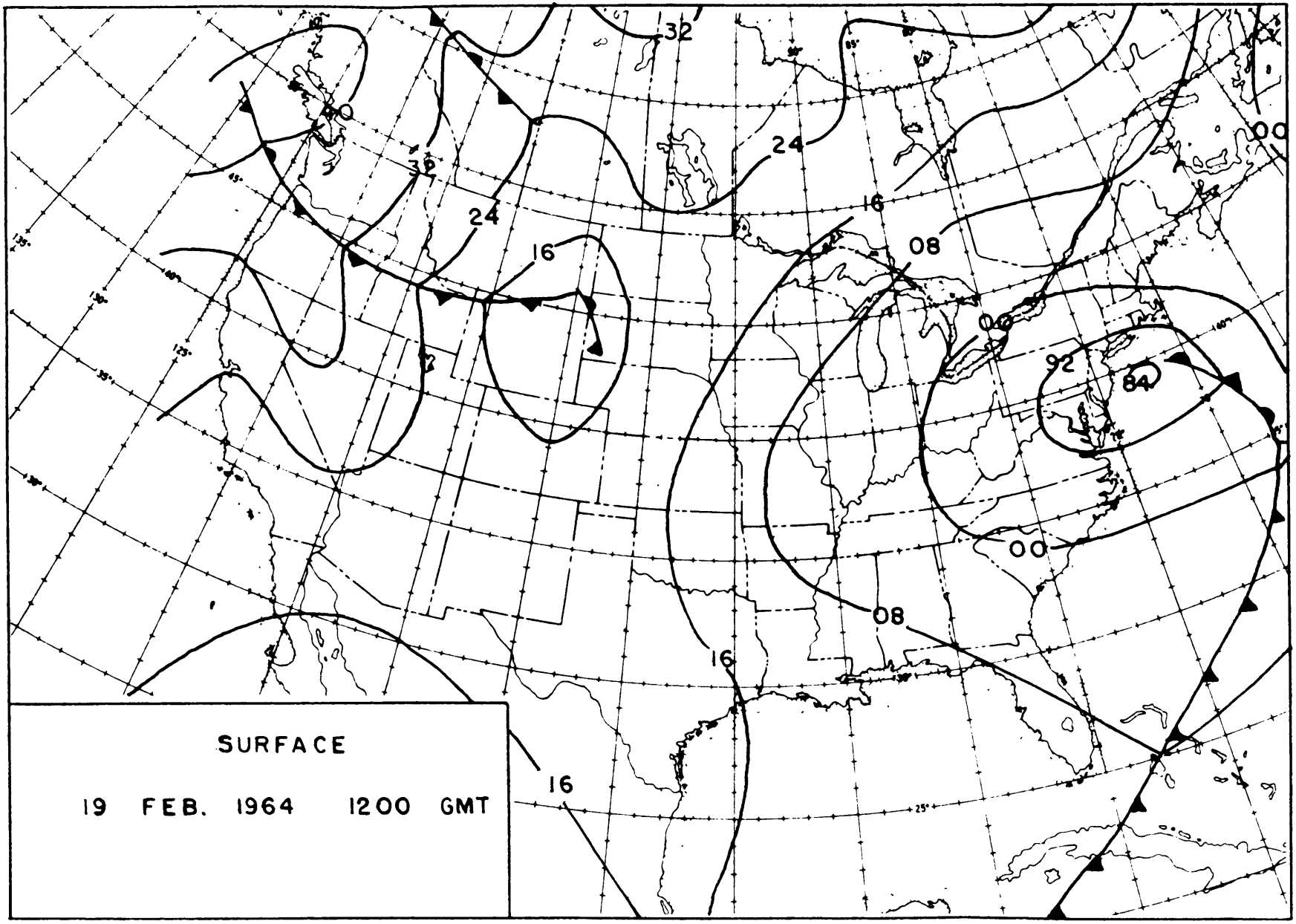

FIGURE 1

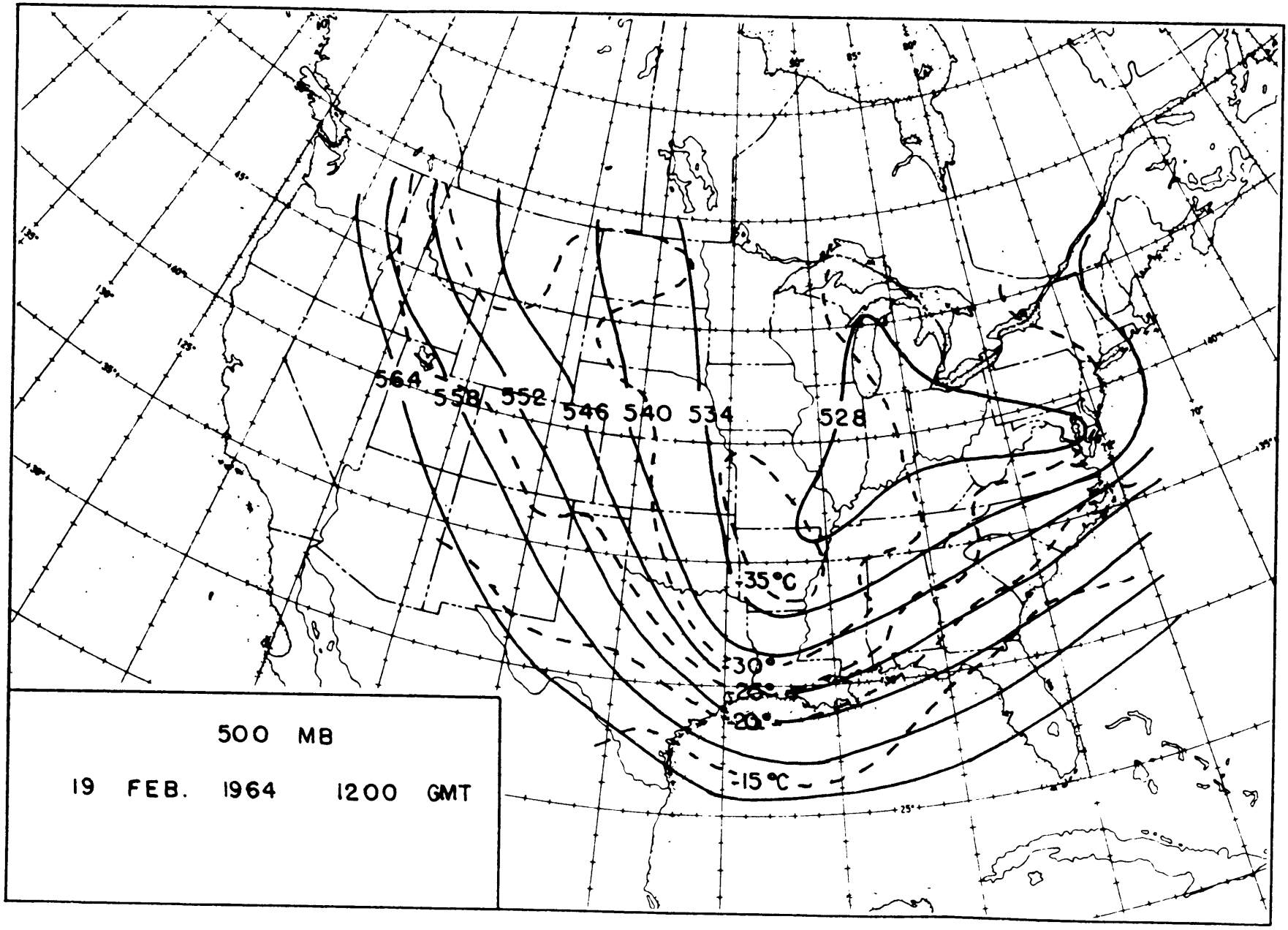
564
558
552
546
540
534
528
-35°C
-30°
-25°
-20°
-15°C
500 MB
19 FEB. 1964 1200 GMT

FIGURE 2

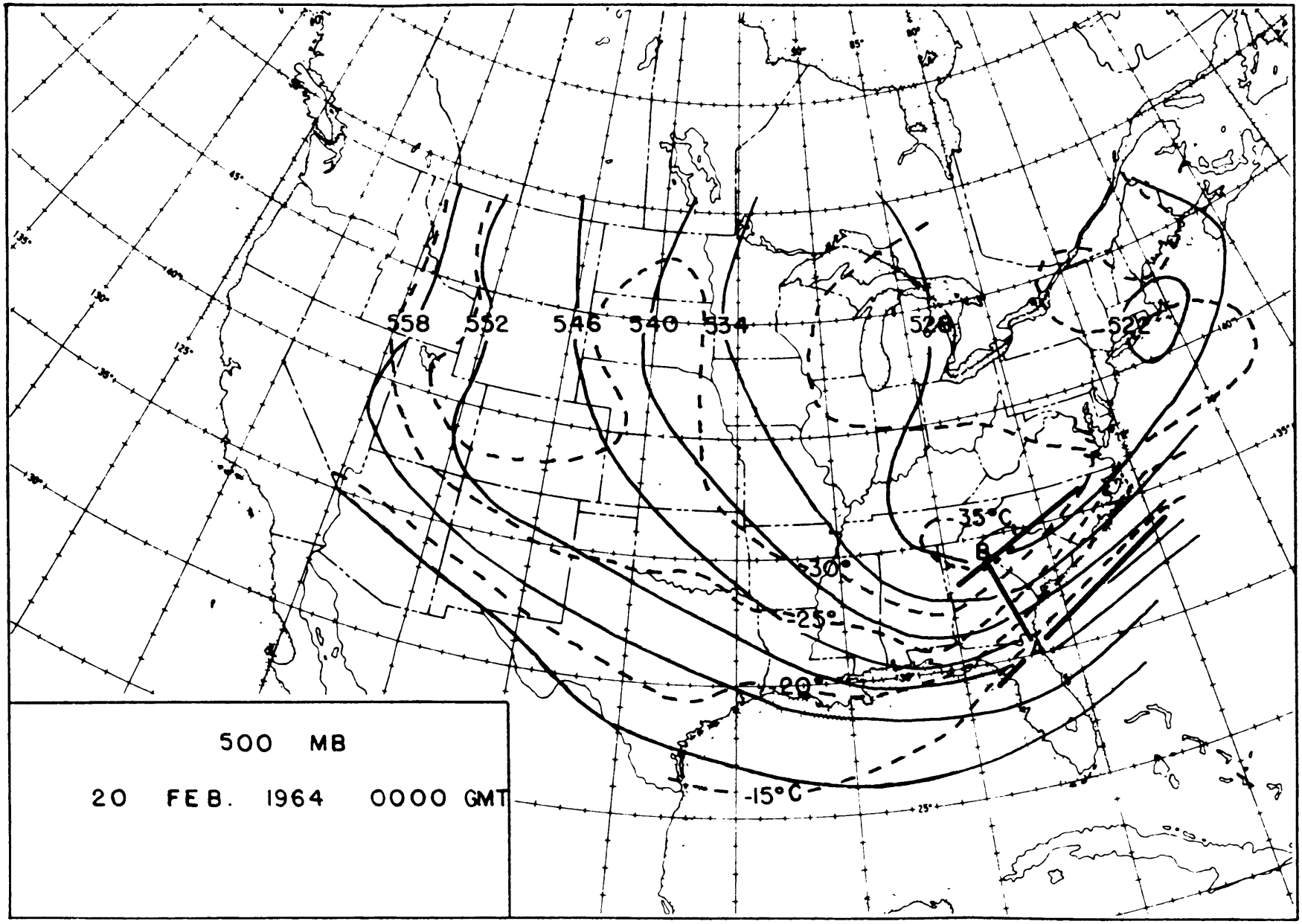
558
552
546
540
534
528
522
-35°C
-30°
-25°
-20°
-15°C
500 MB
20 FEB. 1964 0000 GMT

FIGURE 3

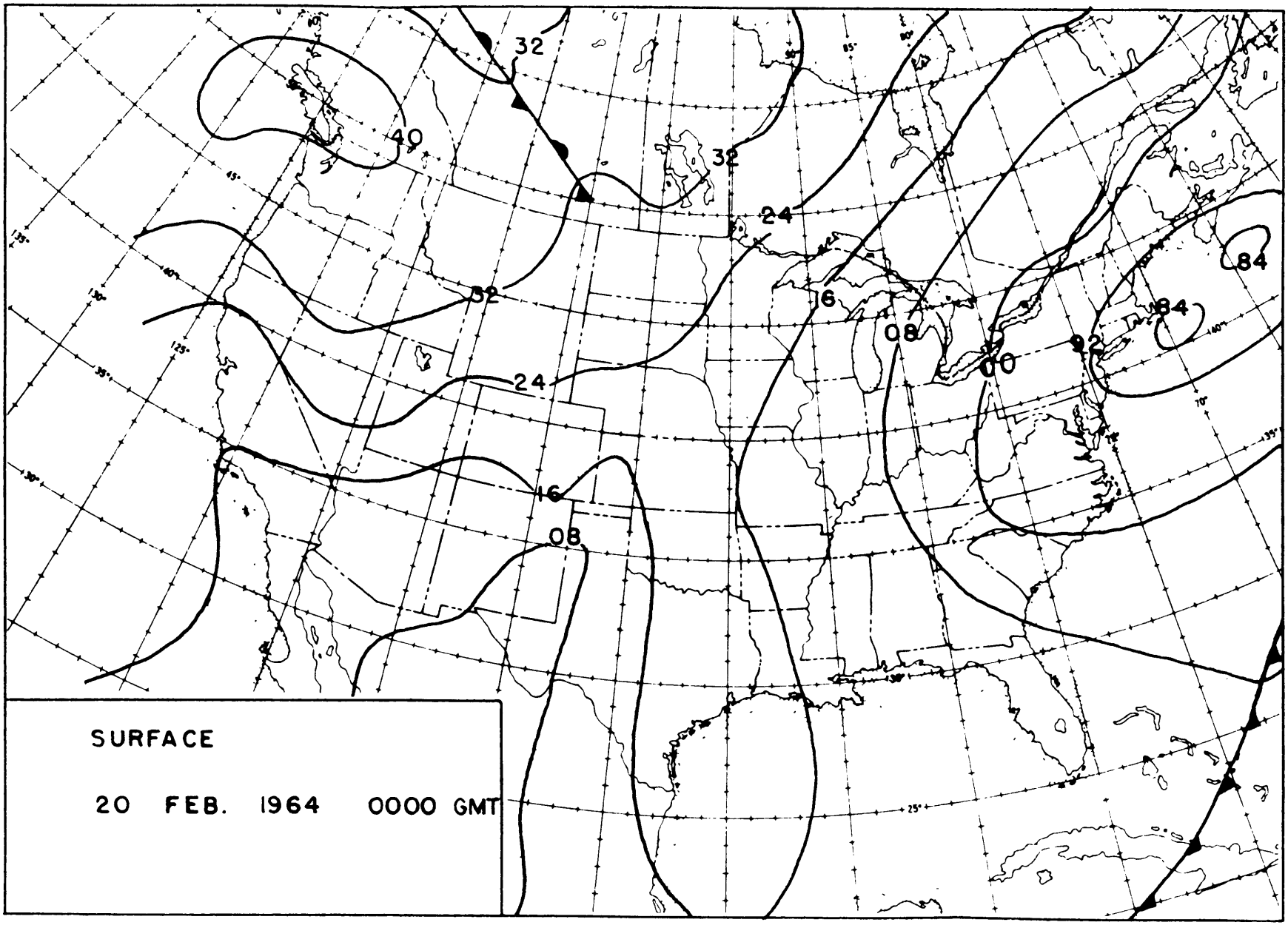
32
40
32
24
32
16
08
00
92
84
84
24
16
08
SURFACE
20 FEB. 1964 0000 GMT

FIGURE 4

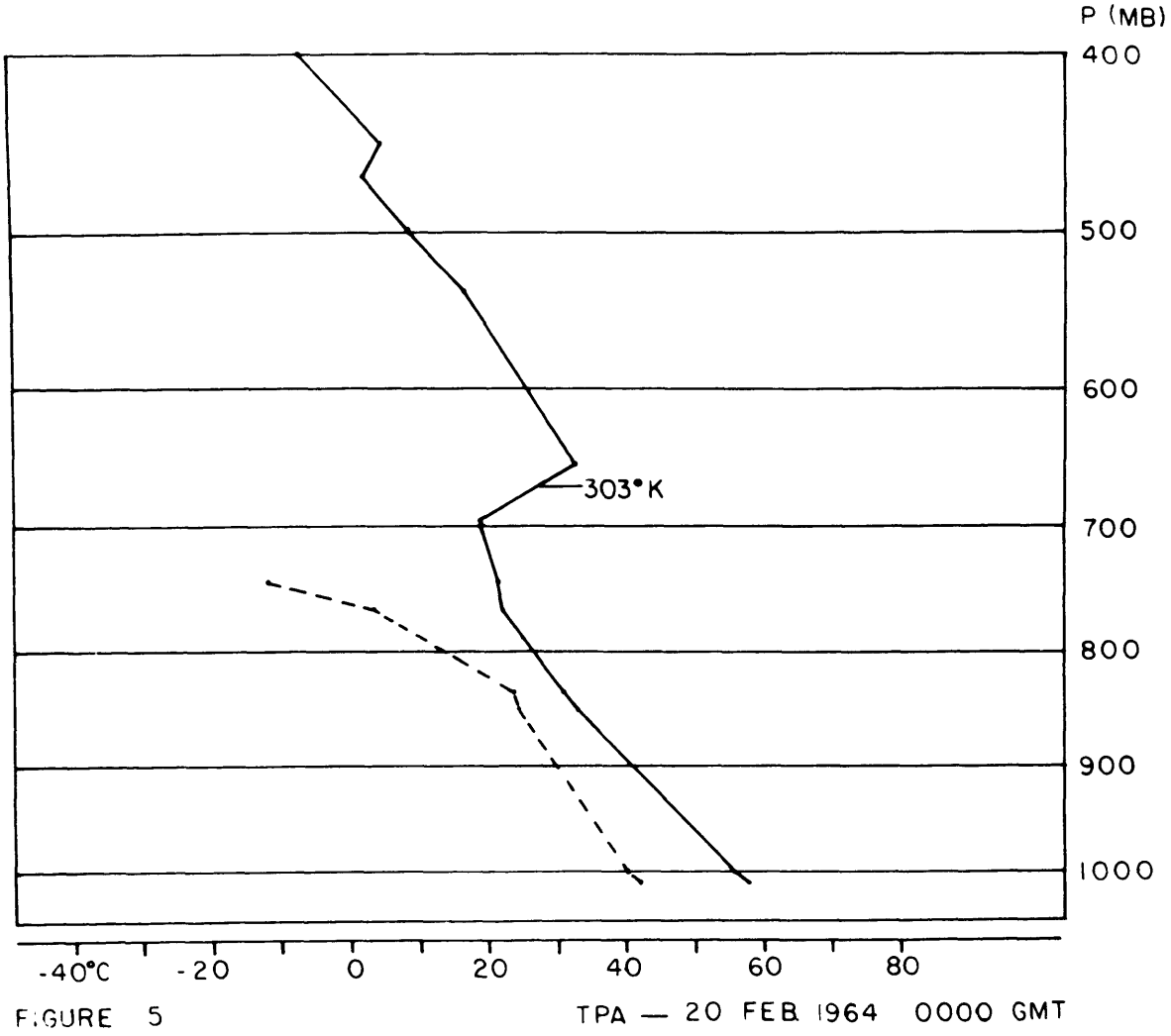

FIGURE 5

TPA — 20 FEB 1964 0000 GMT

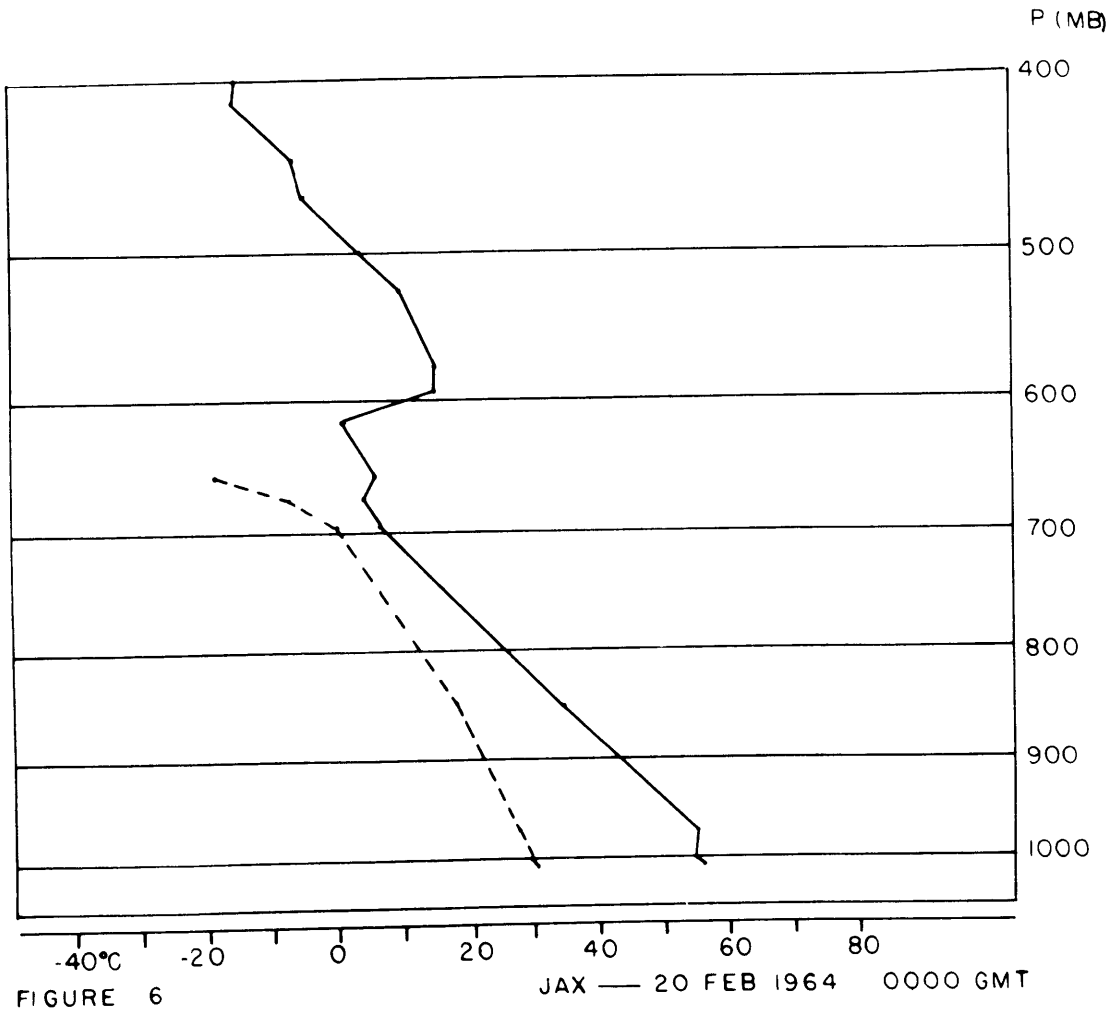
P (MB)
400
500
600
700
800
900
1000
-40°C
-20
0
20
40
60
80
JAX — 20 FEB 1964 0000 GMT

FIGURE 6

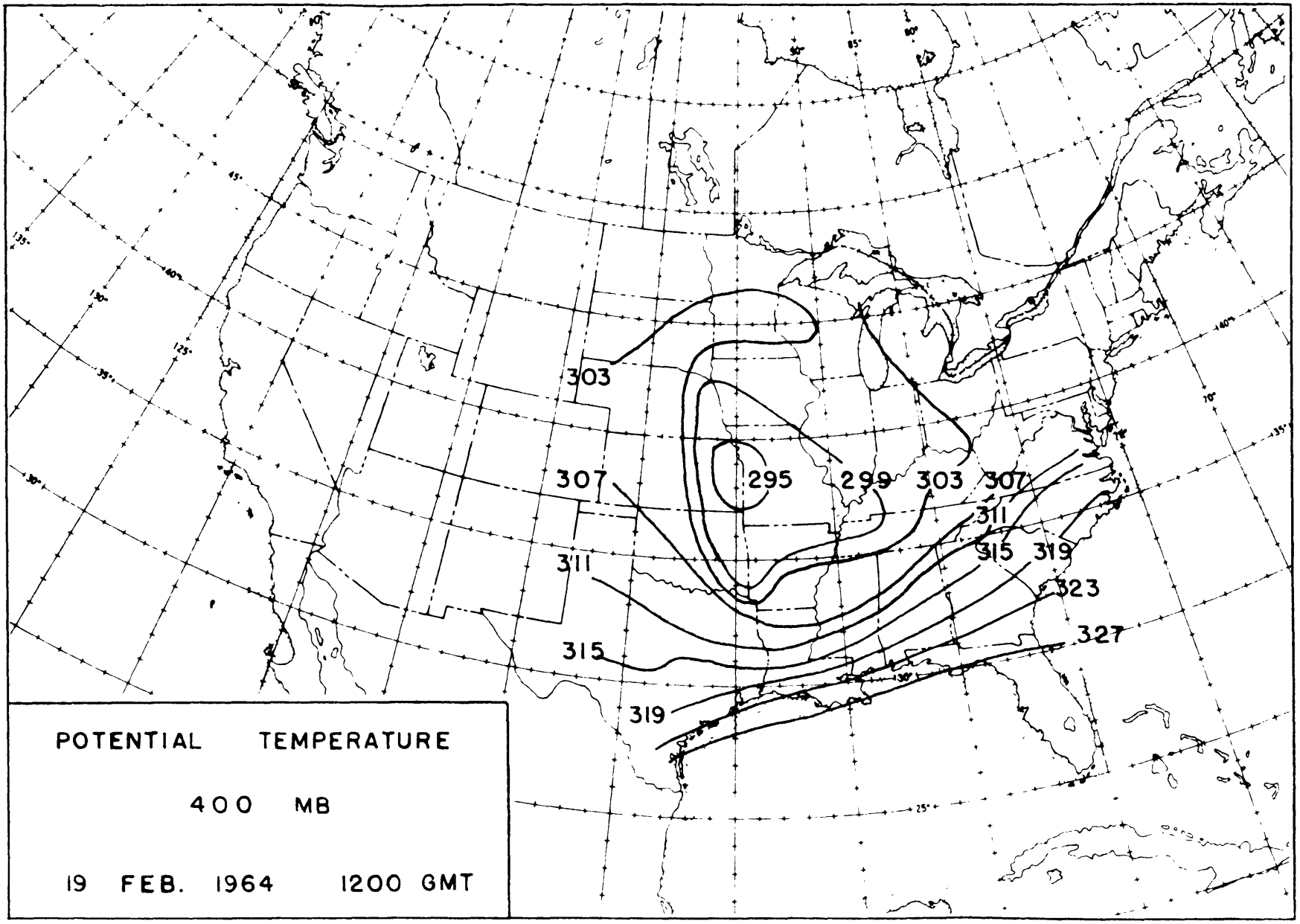
303
307
295
299
303
307
311
315
319
323
327
311
315
319
POTENTIAL TEMPERATURE
400 MB
19 FEB. 1964 1200 GMT

FIGURE 7

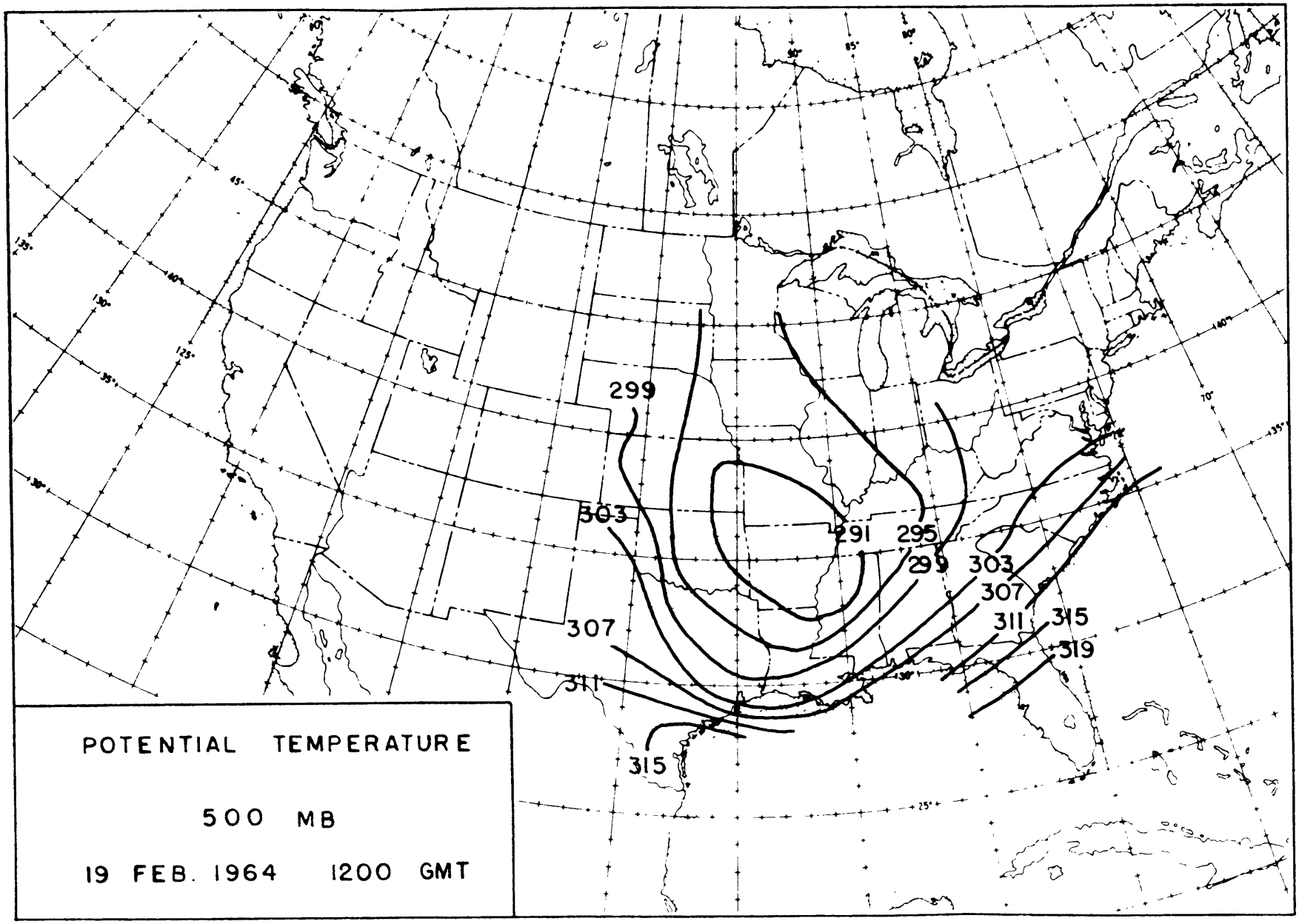
299
303
291
295
299
303
307
311
315
319
307
311
315
POTENTIAL TEMPERATURE
500 MB
19 FEB. 1964 1200 GMT

FIGURE 8

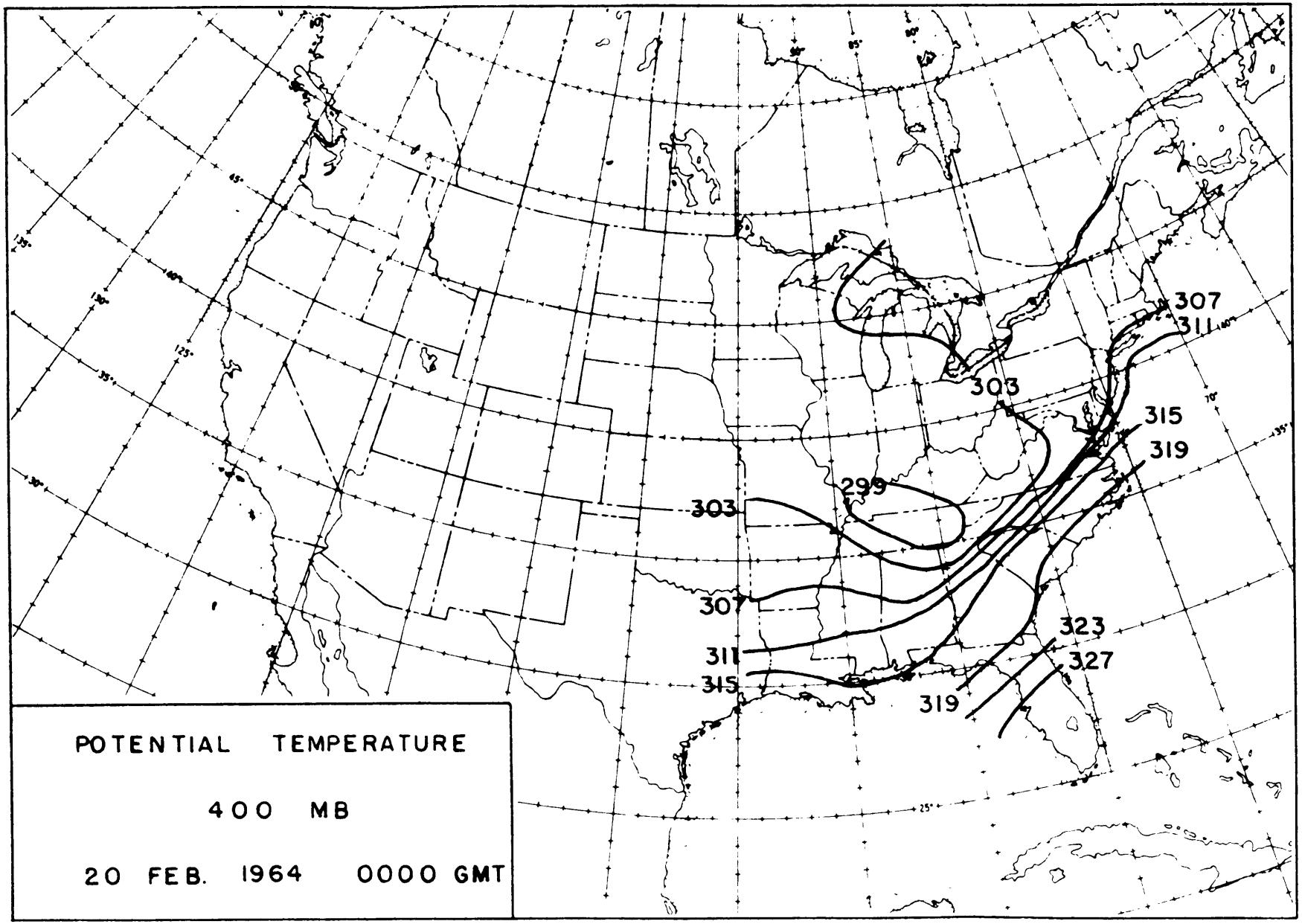
307
311
303
315
319
299
303
307
323
311
327
315
319
POTENTIAL TEMPERATURE
400 MB
20 FEB. 1964 0000 GMT

FIGURE 9

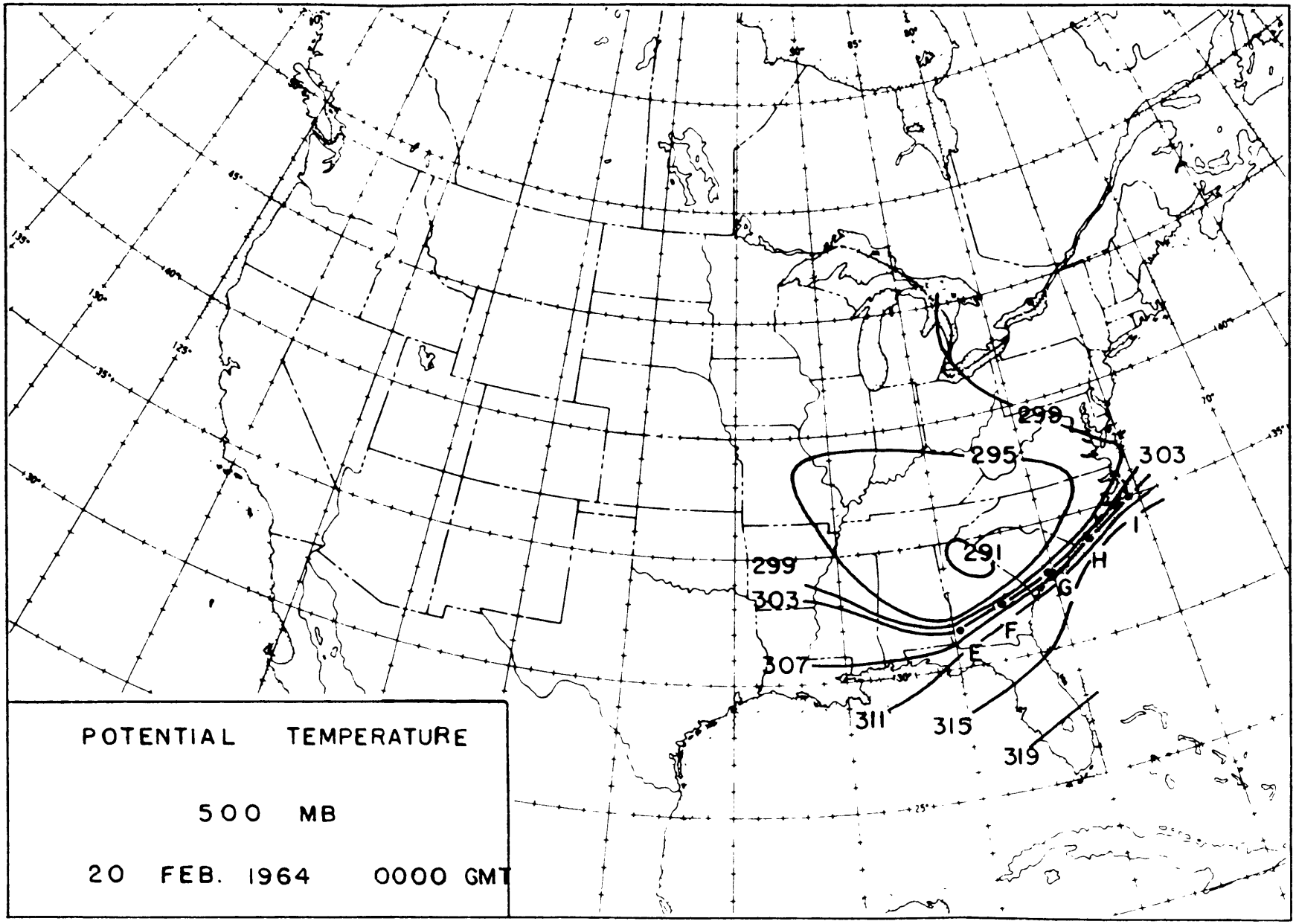
POTENTIAL TEMPERATURE
500 MB
20 FEB. 1964 0000 GMT
299
295
303
291
I
H
G
F
E
307
311
315
319

FIGURE 10

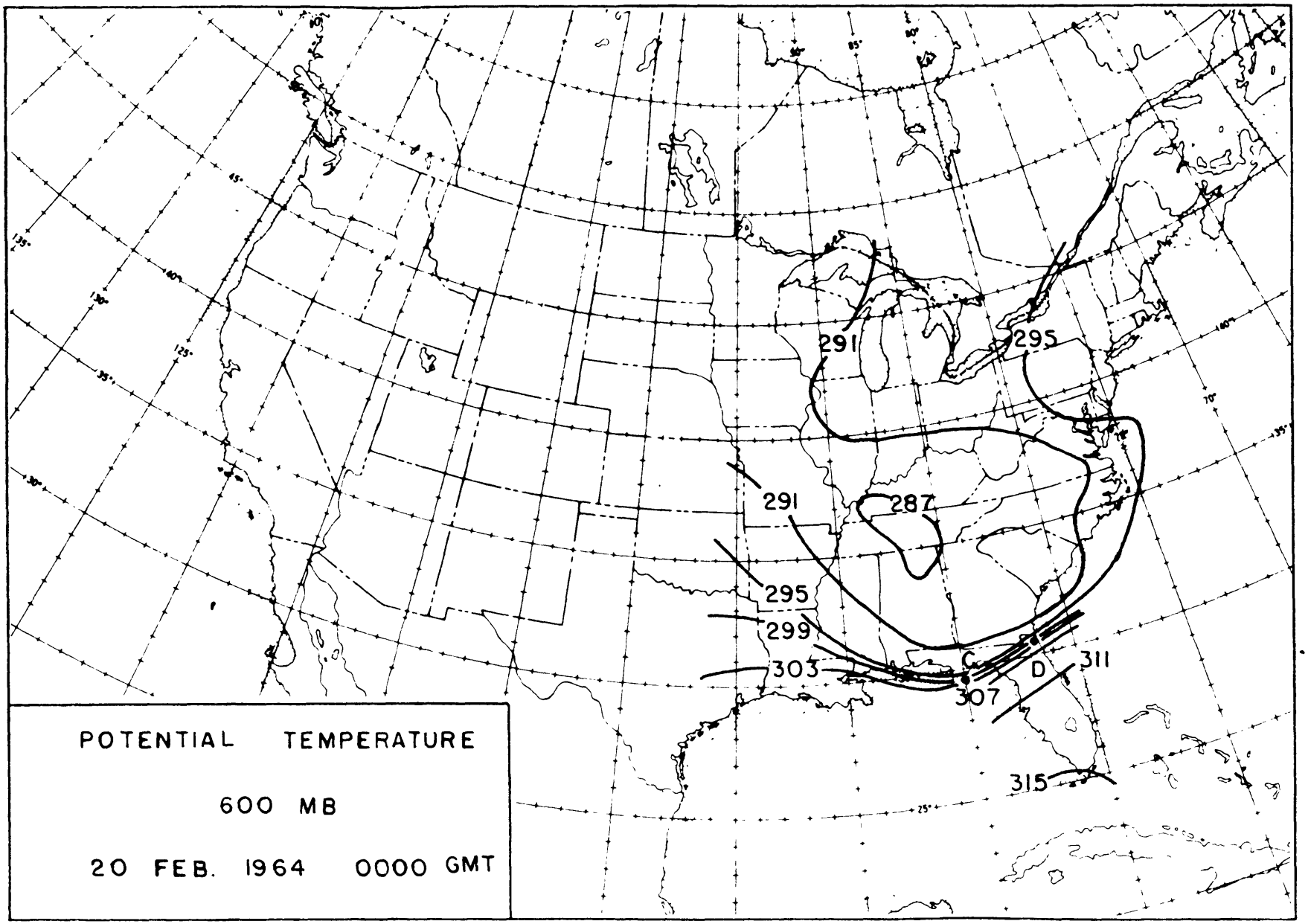
291
295
291
287
295
299
303
C
D
311
307
315
POTENTIAL TEMPERATURE
600 MB
20 FEB. 1964 0000 GMT

FIGURE 11

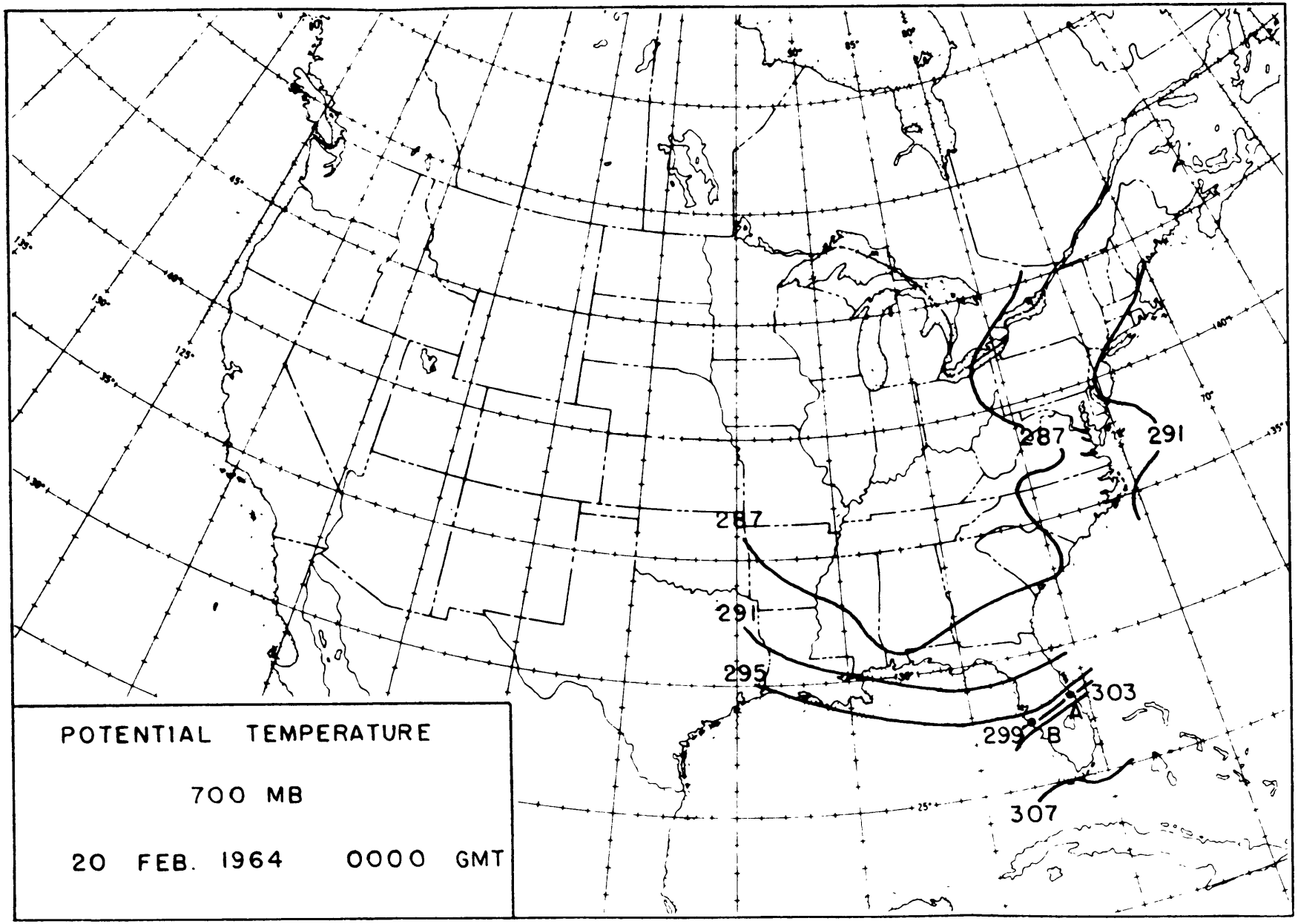
POTENTIAL TEMPERATURE
700 MB
20 FEB. 1964 0000 GMT
287
291
287
291
295
303
299
B
307

FIGURE 12

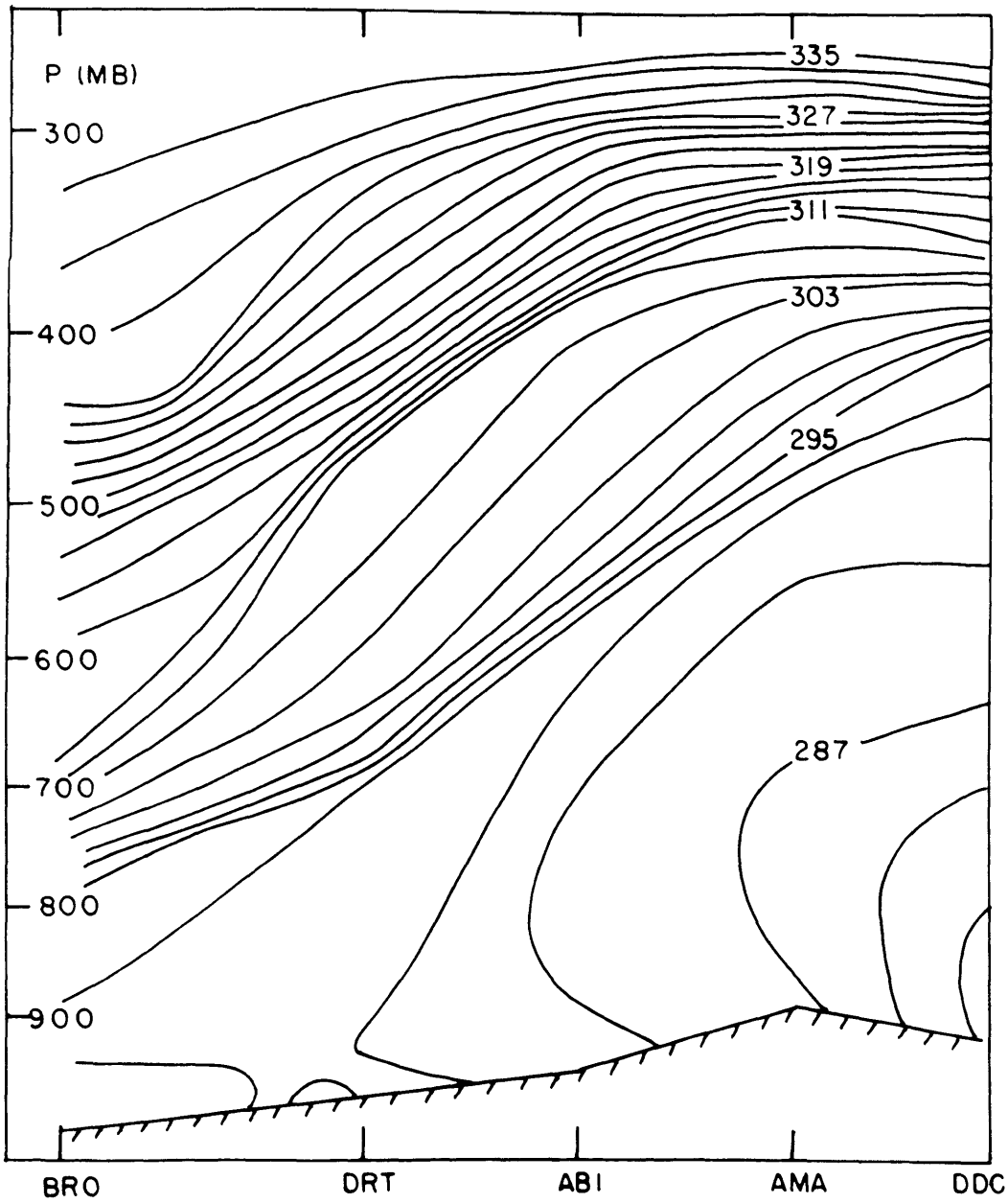

FIGURE 13

19 FEB. 1964 0000 GMT

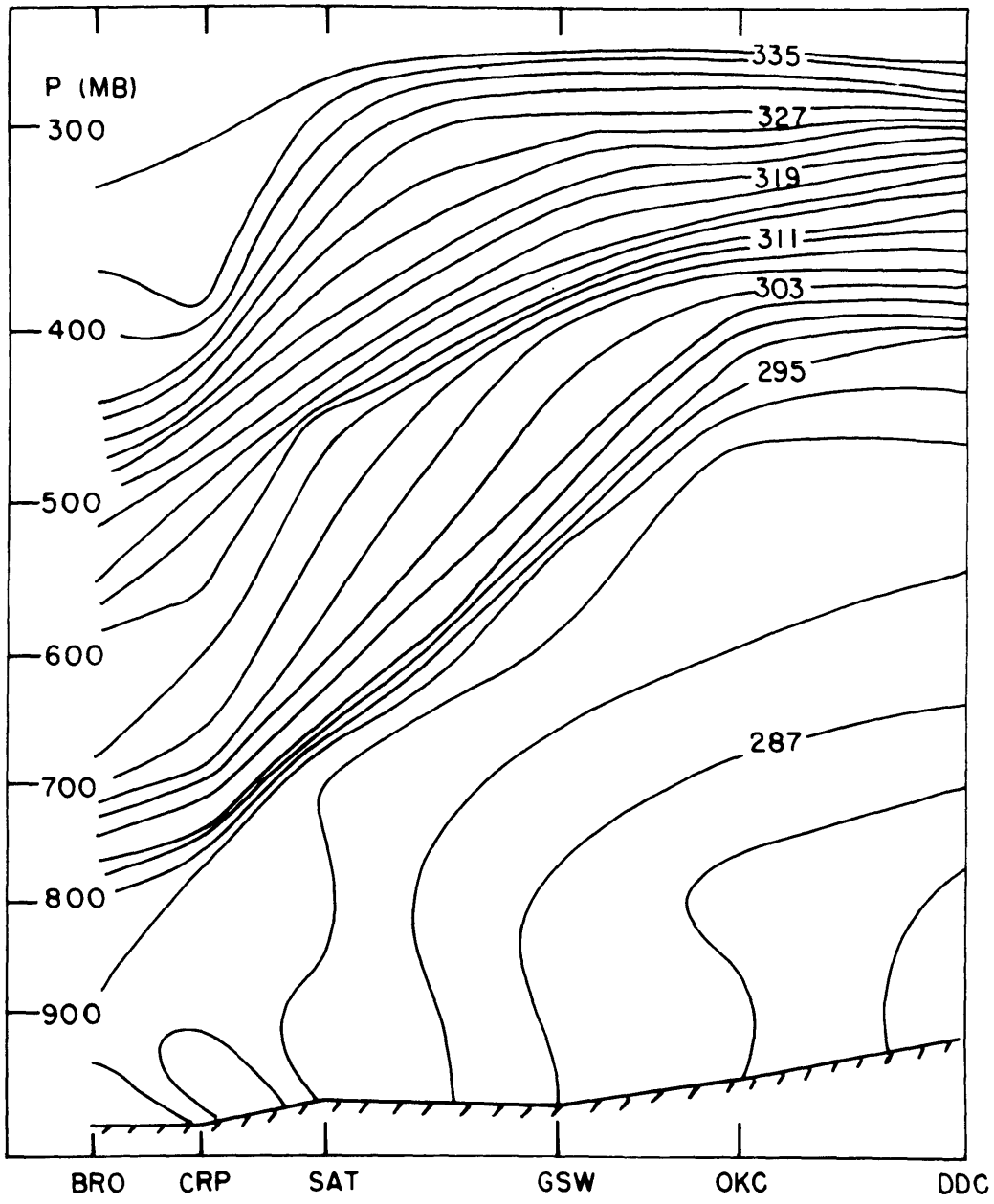

FIGURE 14 19 FEB. 1964 0000 GMT

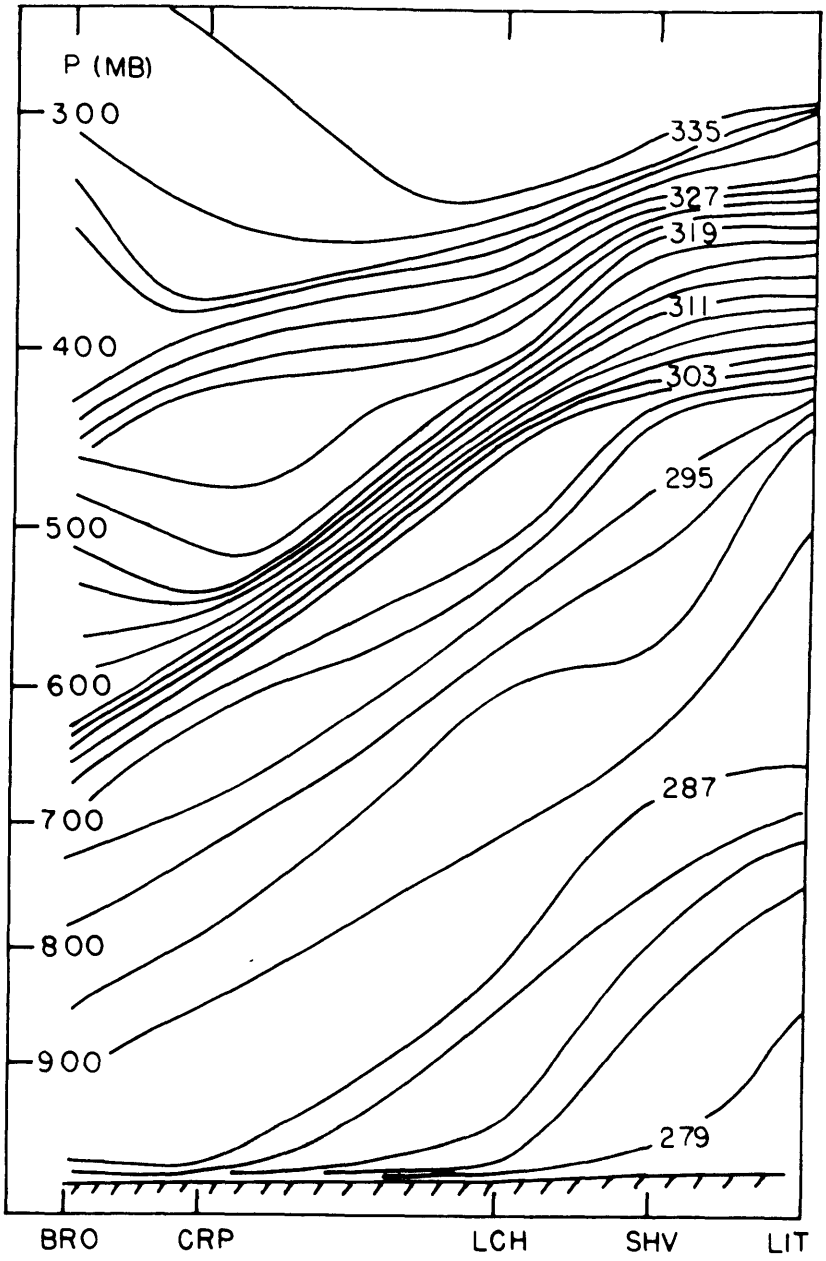

FIGURE 15 19 FEB. 1964 1200 GMT

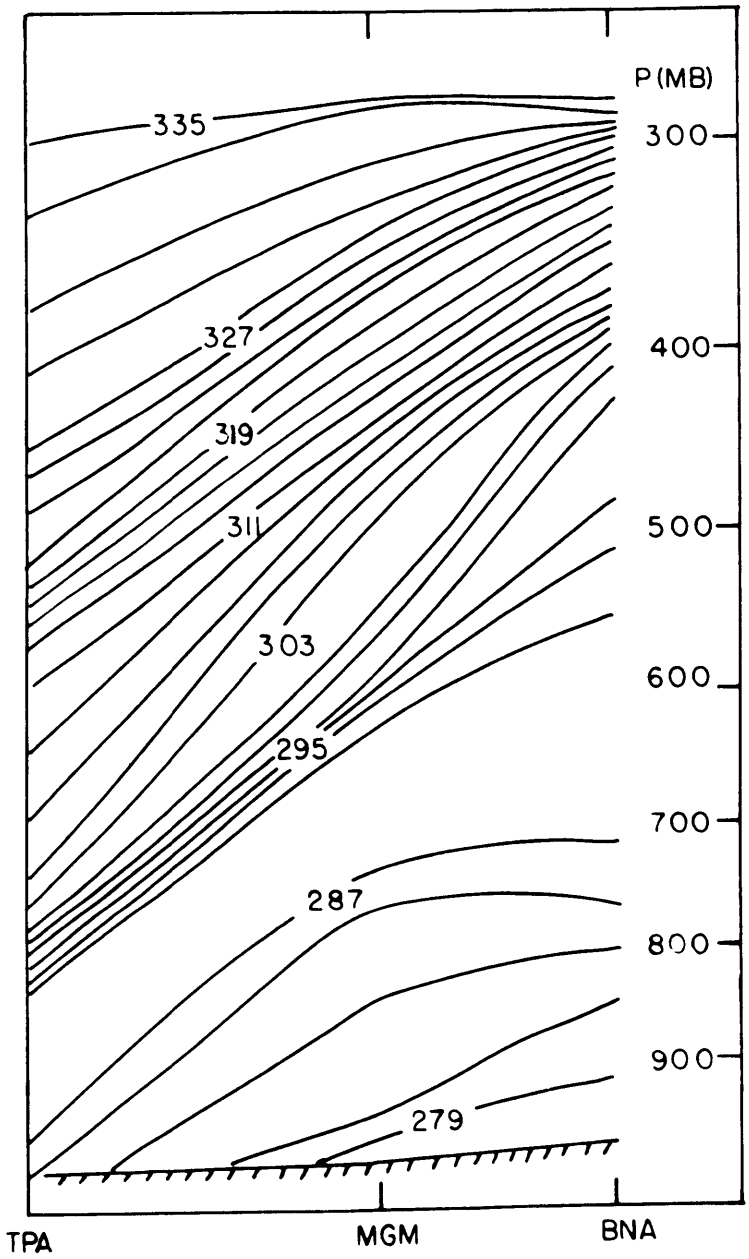

FIGURE 16 19 FEB. 1964 1200 GMT

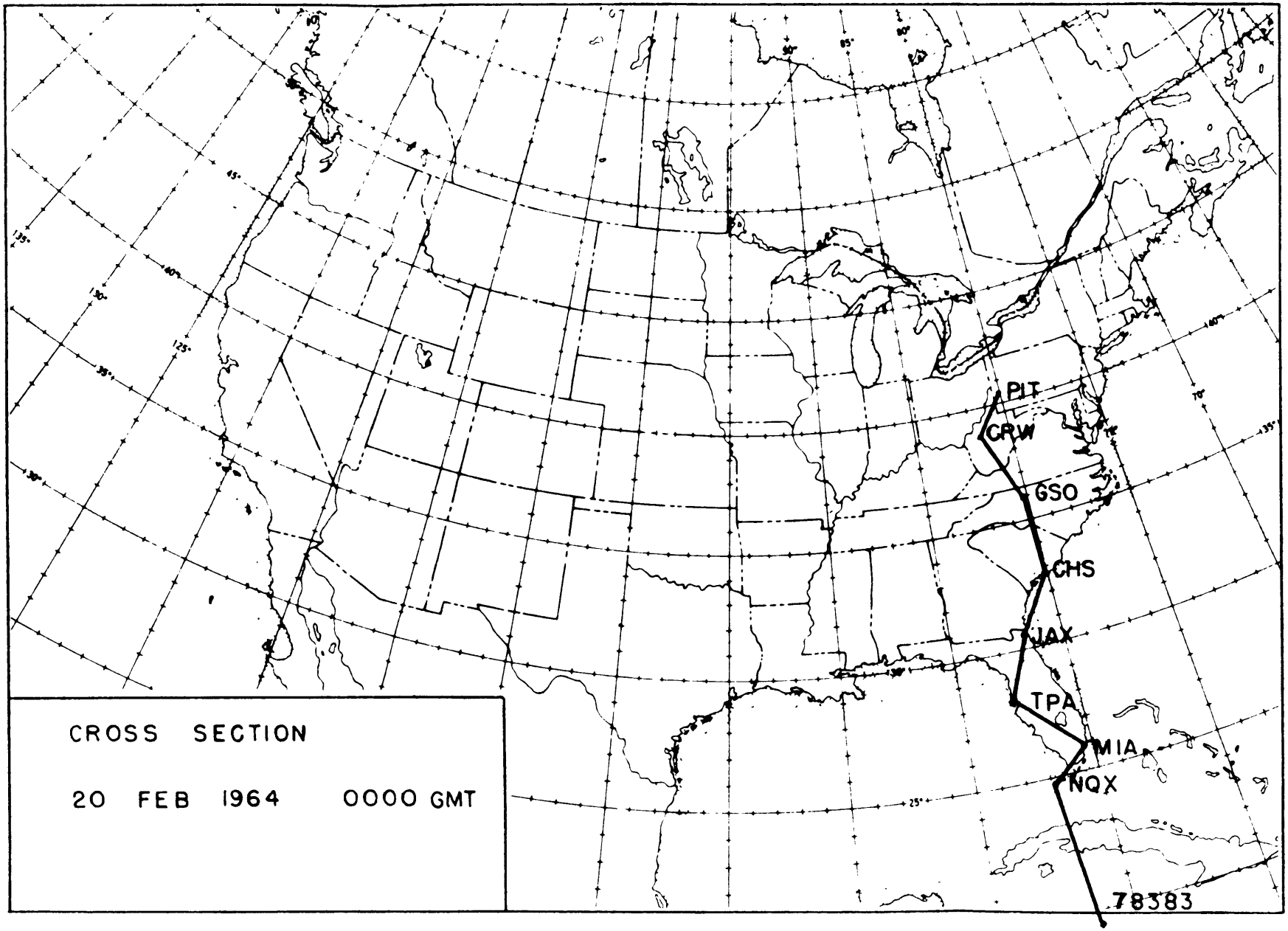
PIT
CRW
GSO
CHS
JAX
TPA
MIA
NQX
78383
CROSS SECTION
20 FEB 1964 0000 GMT

FIGURE 17

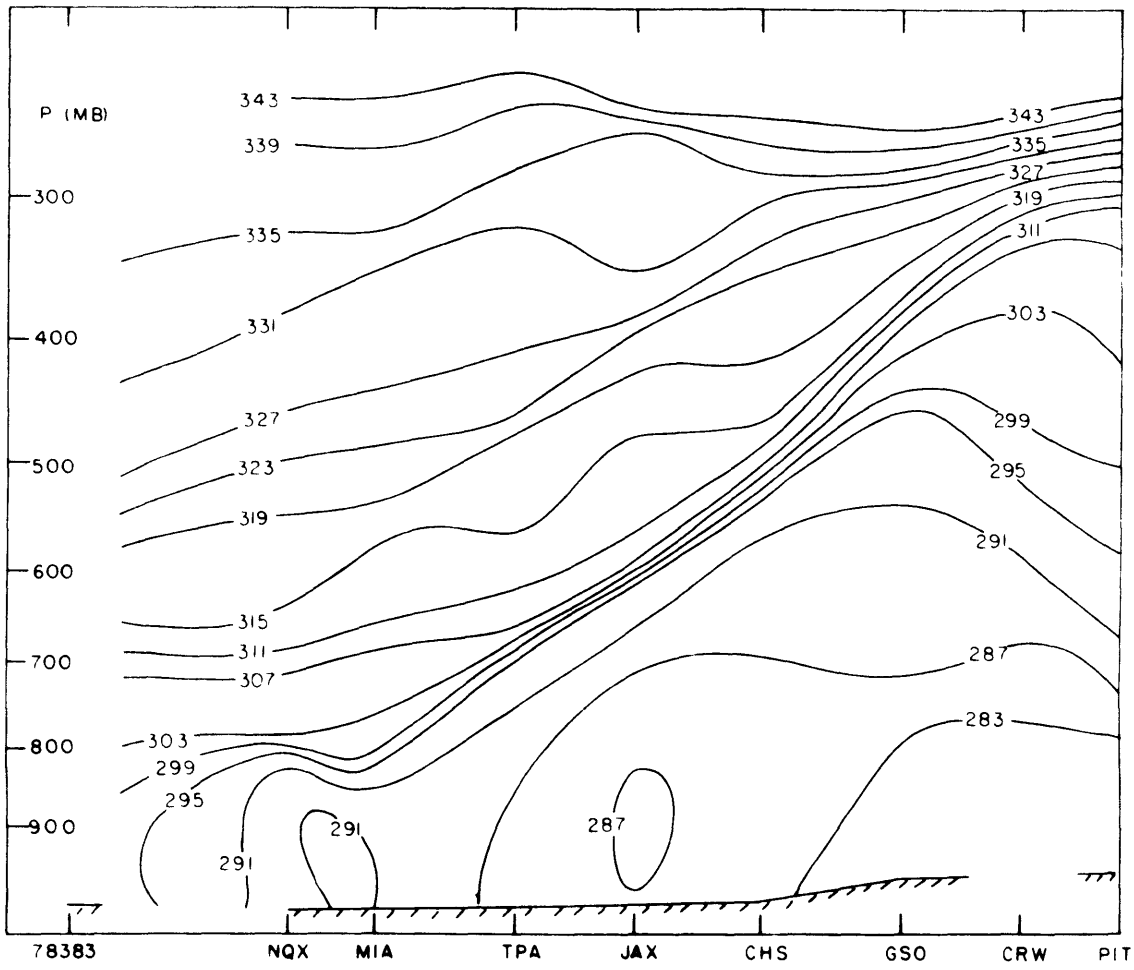

FIGURE 18

20 FEB 1964 0000 GMT

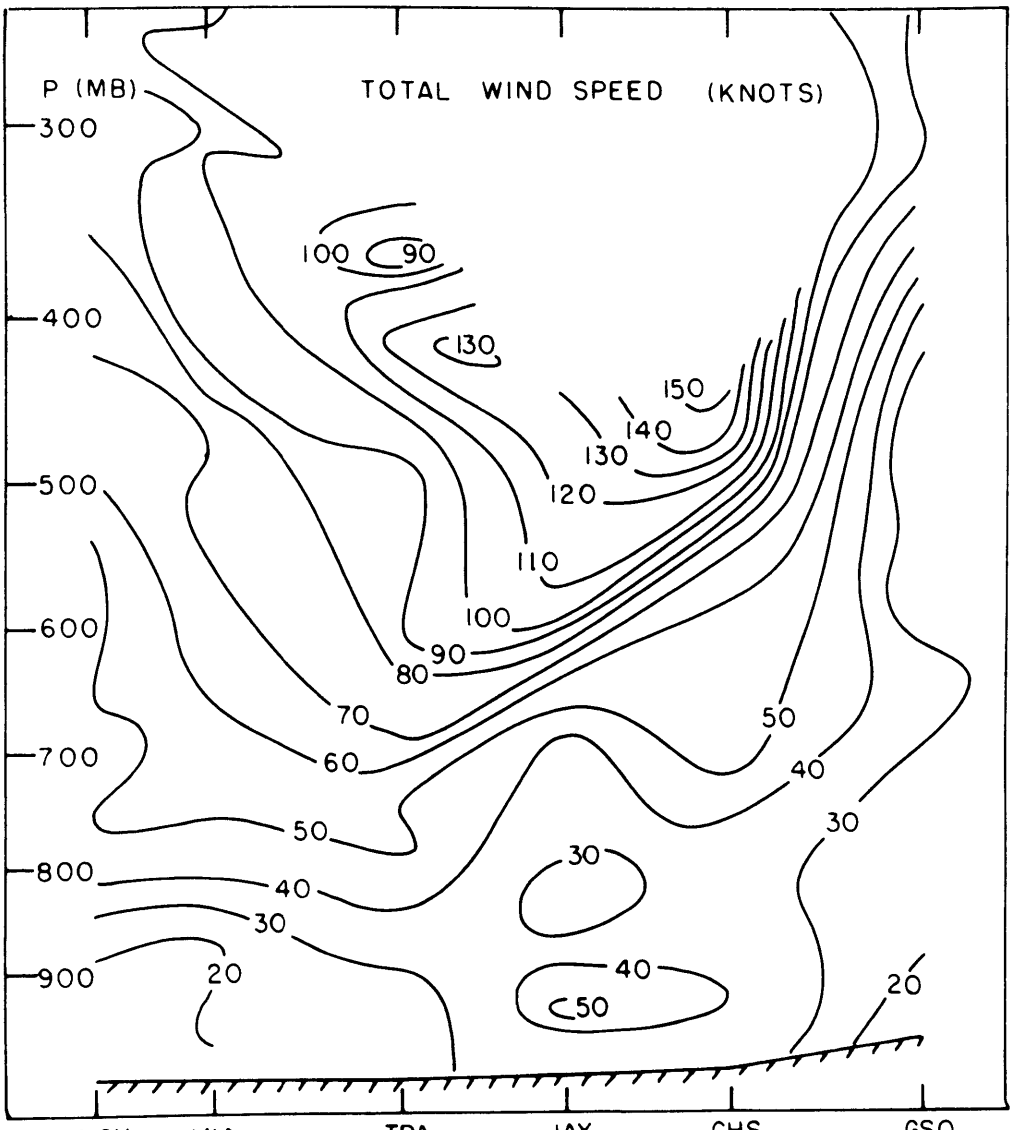

FIGURE 19 20 FEB. 1964 0000 GMT

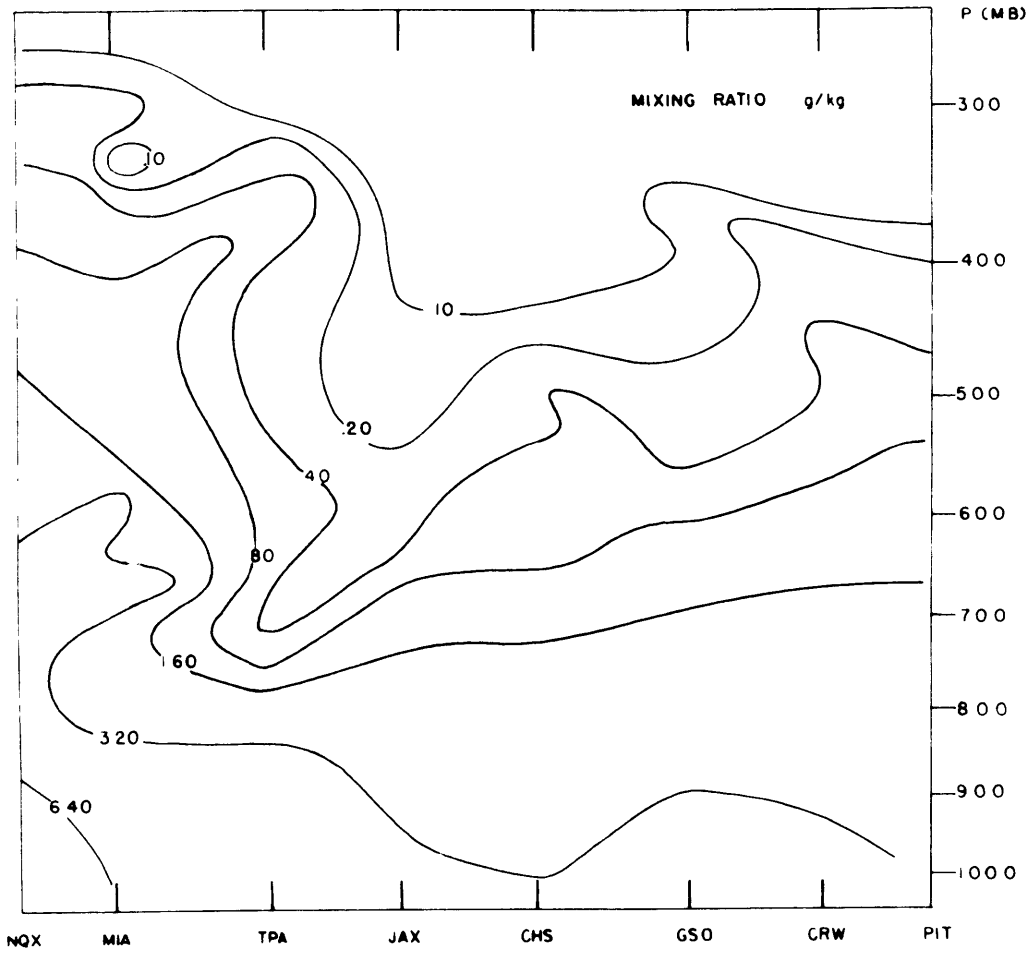
P (MB)
MIXING RATIO g/kg
10
10
20
40
80
160
320
640
300
400
500
600
700
800
900
1000
NQX
MIA
TPA
JAX
CHS
GSO
CRW
PIT

FIGURE 20

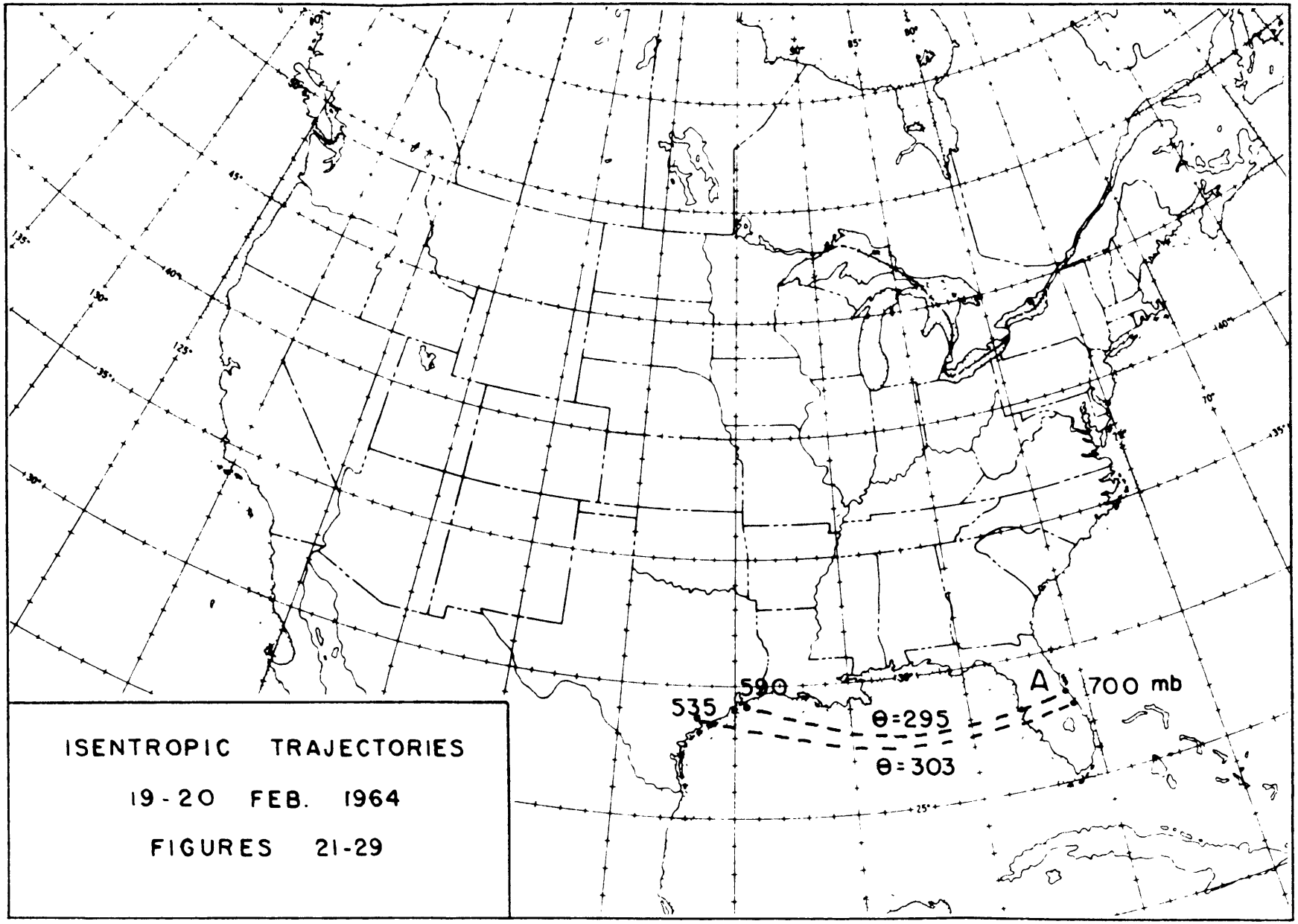
ISENTROPIC TRAJECTORIES
19-20 FEB. 1964
FIGURES 21-29
535
590
A
700 mb
θ=295
θ=303

FIGURE 21

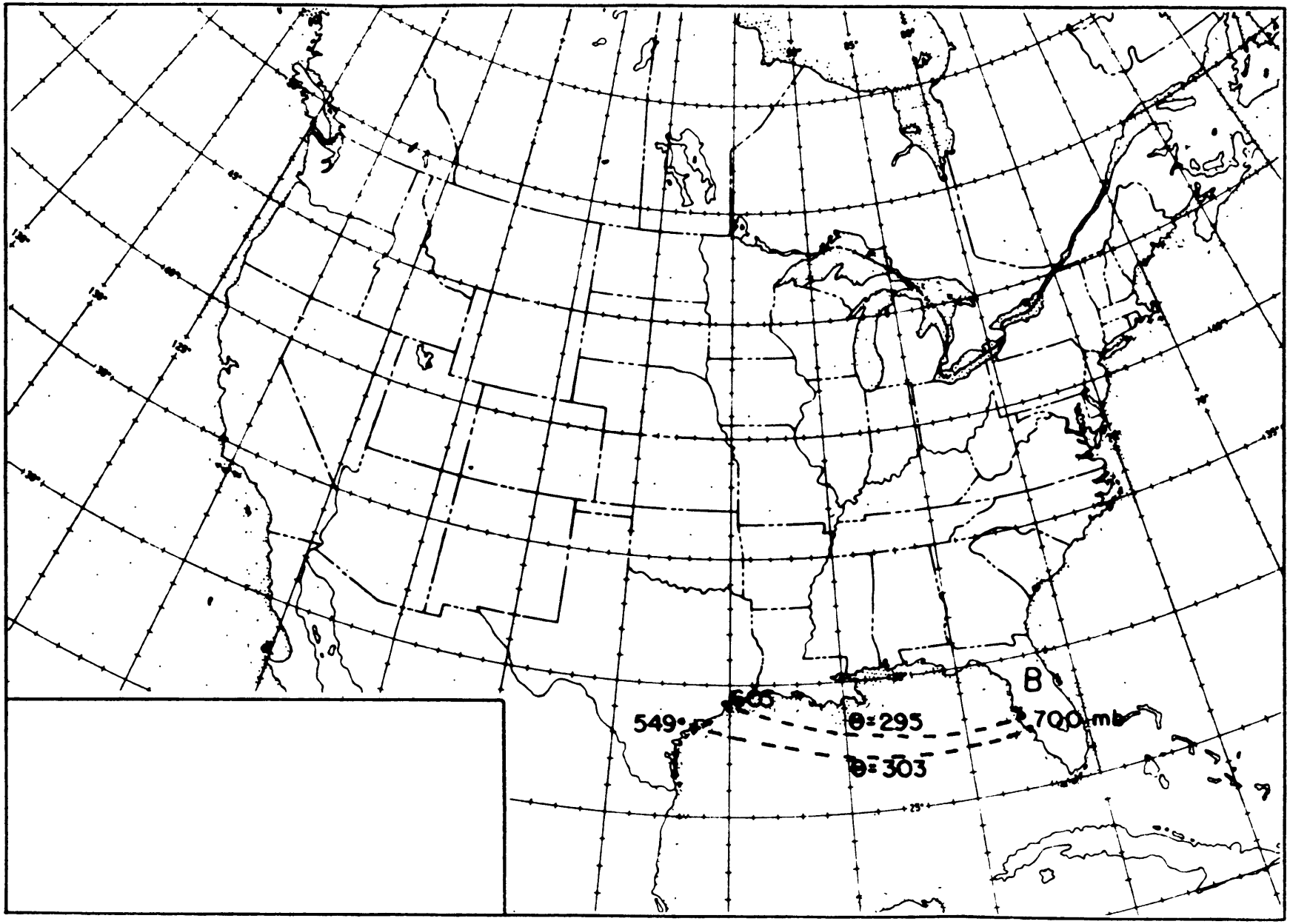

FIGURE 22

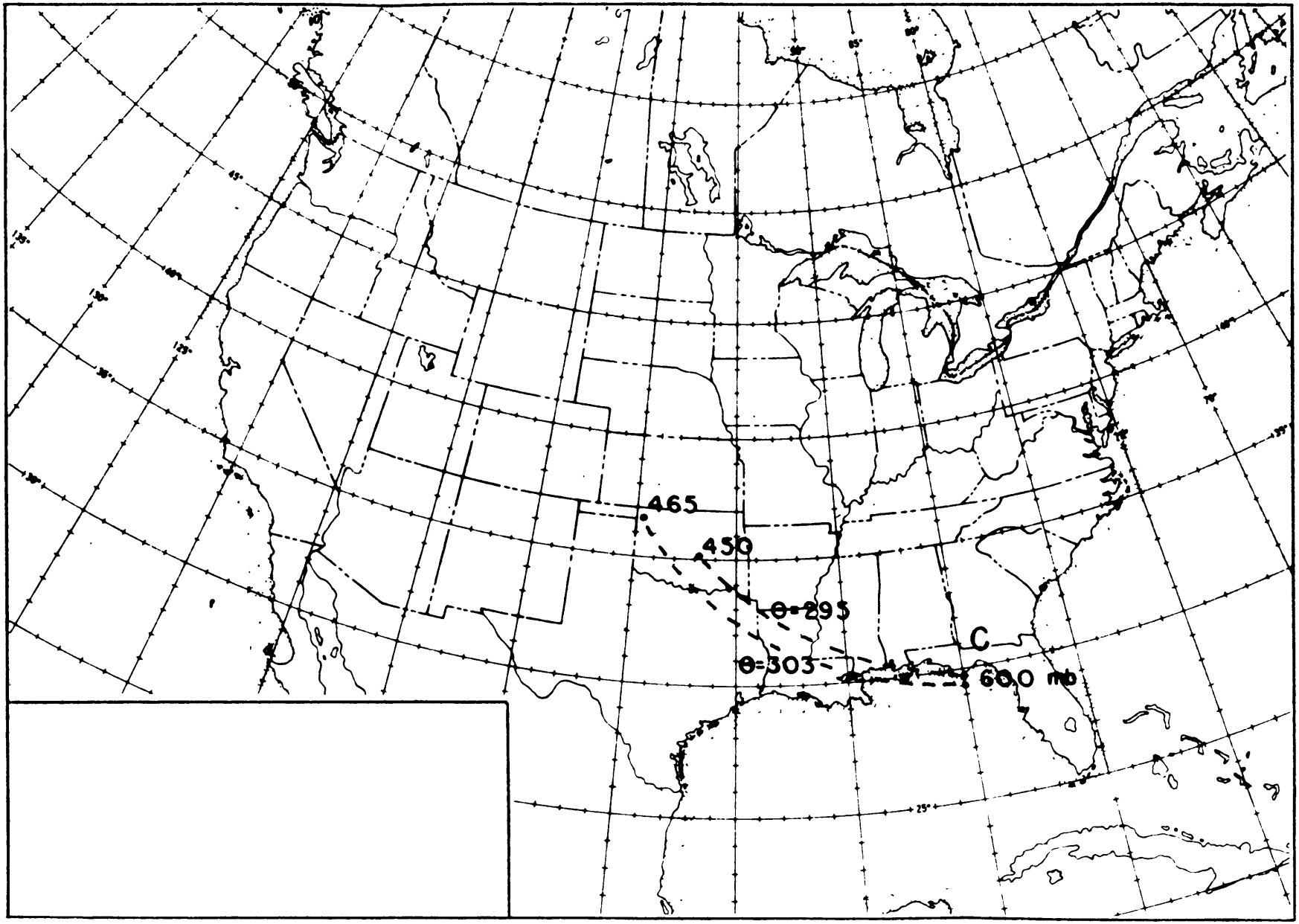

FIGURE 23

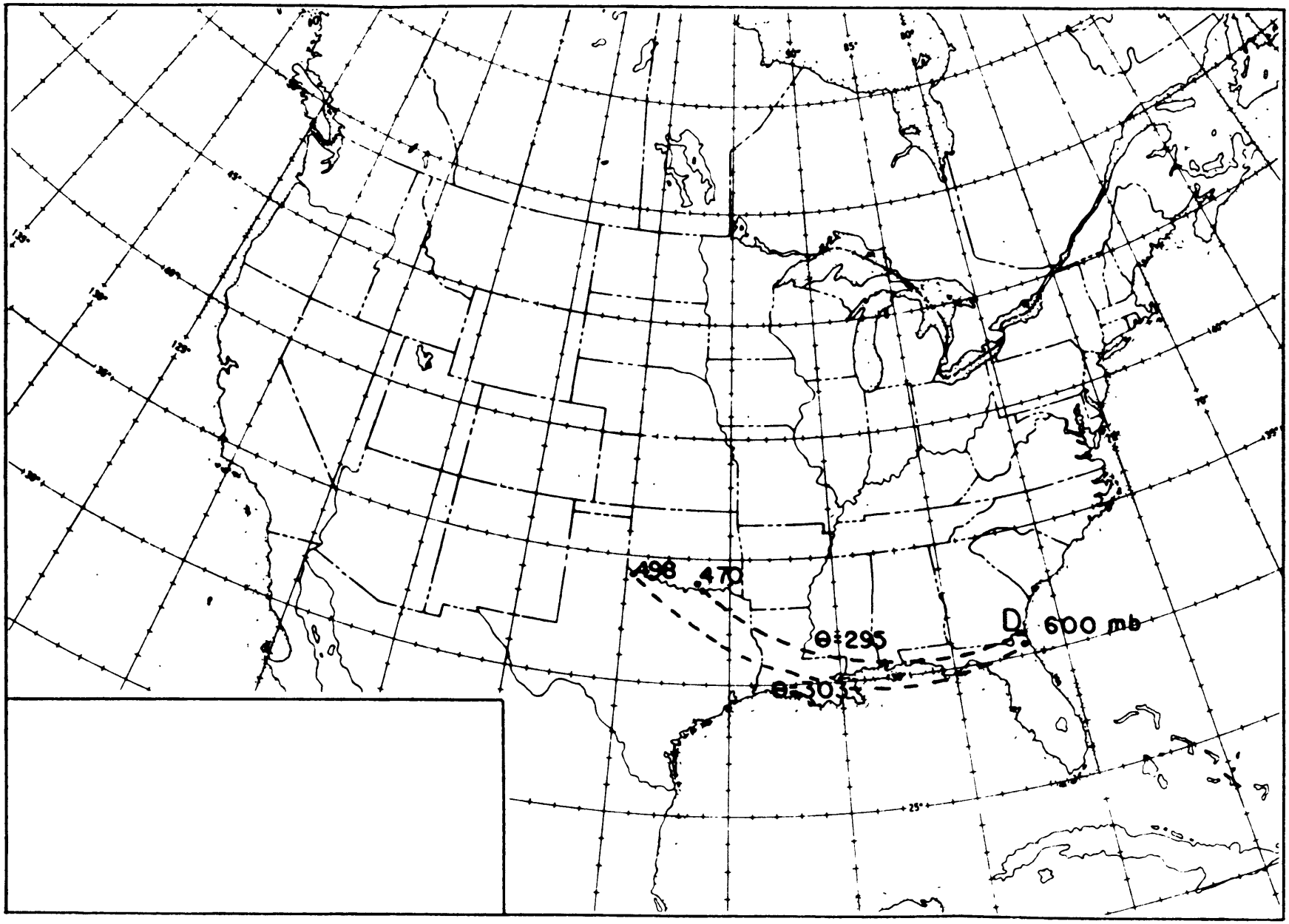

FIGURE 24

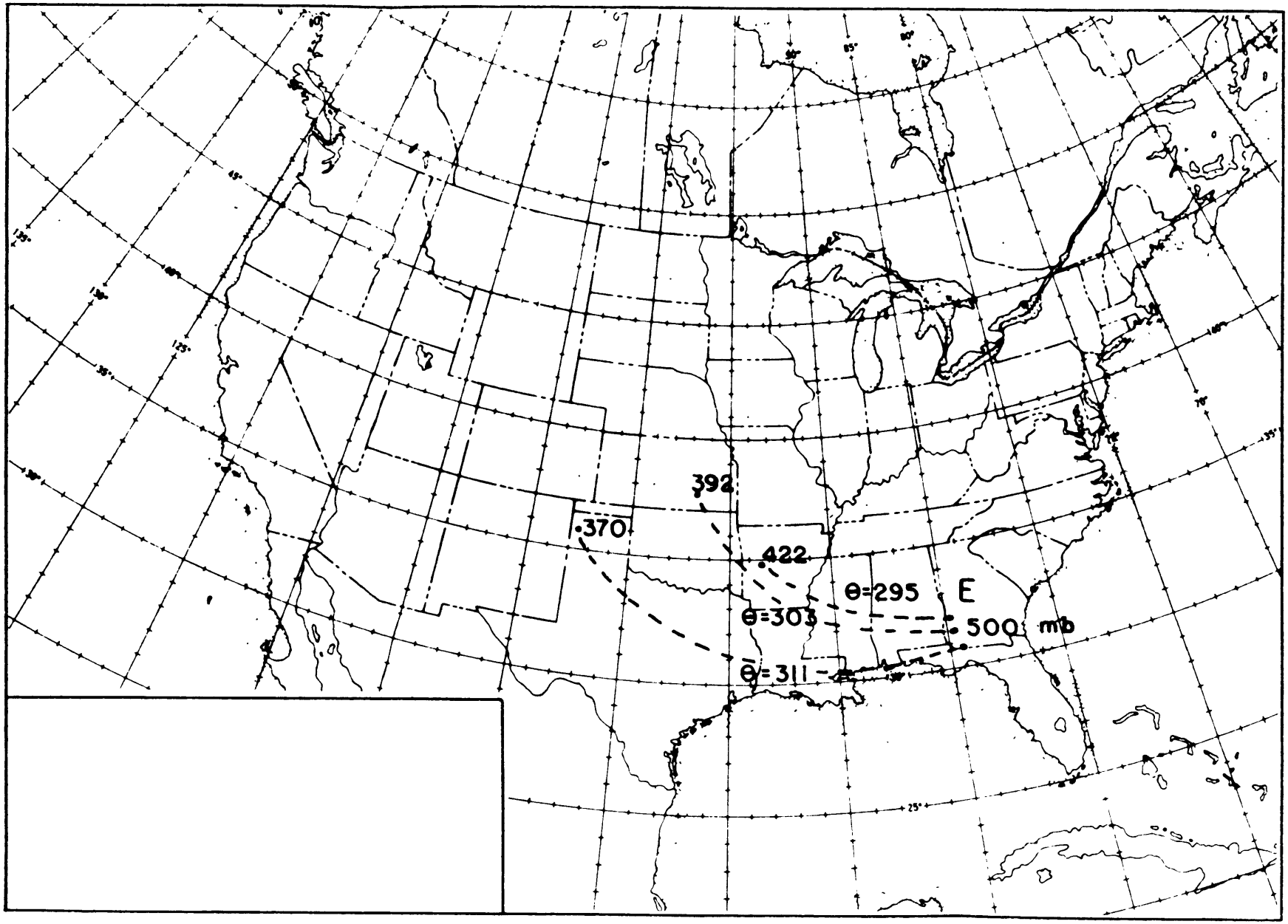

FIGURE 25

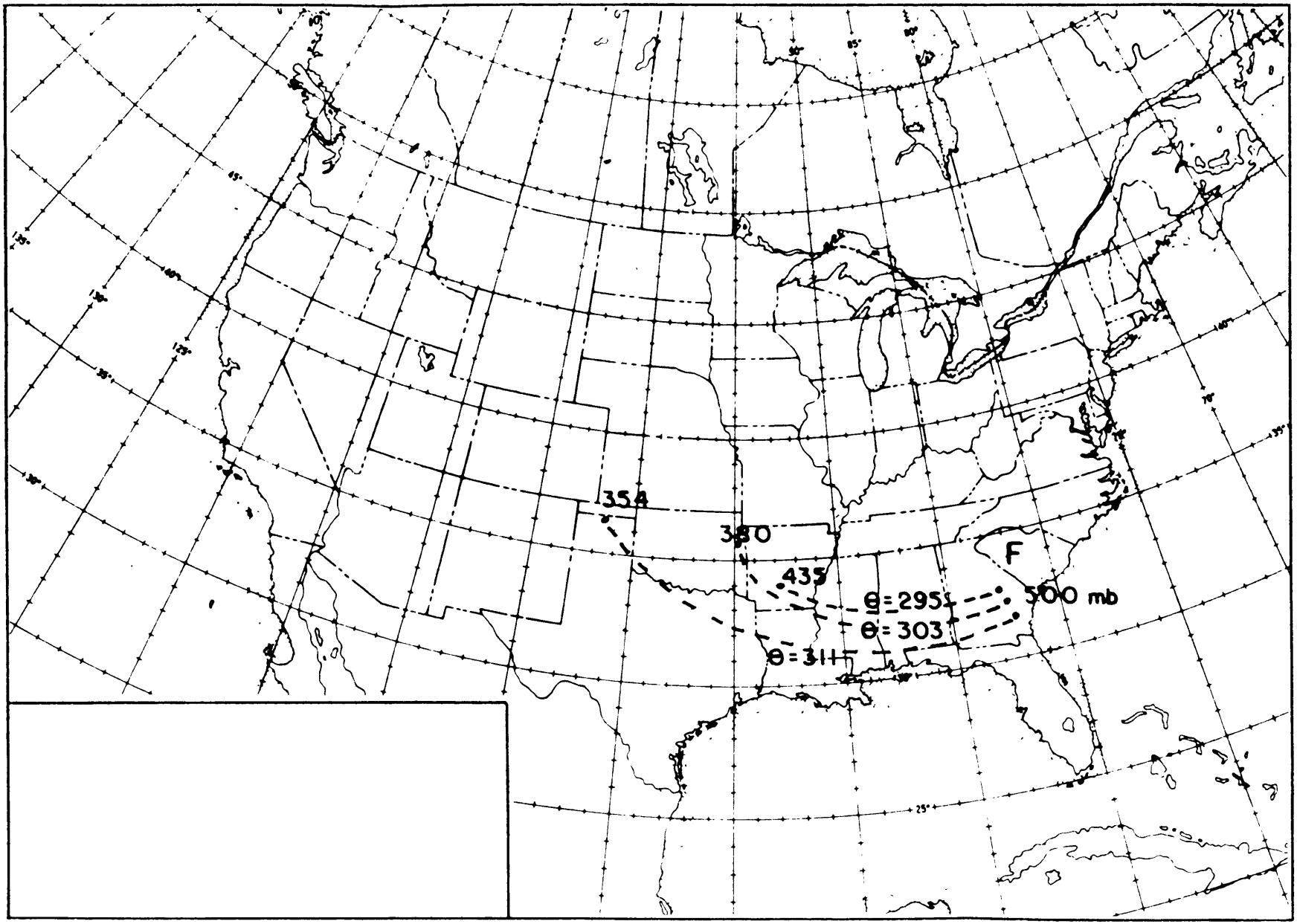

FIGURE 26

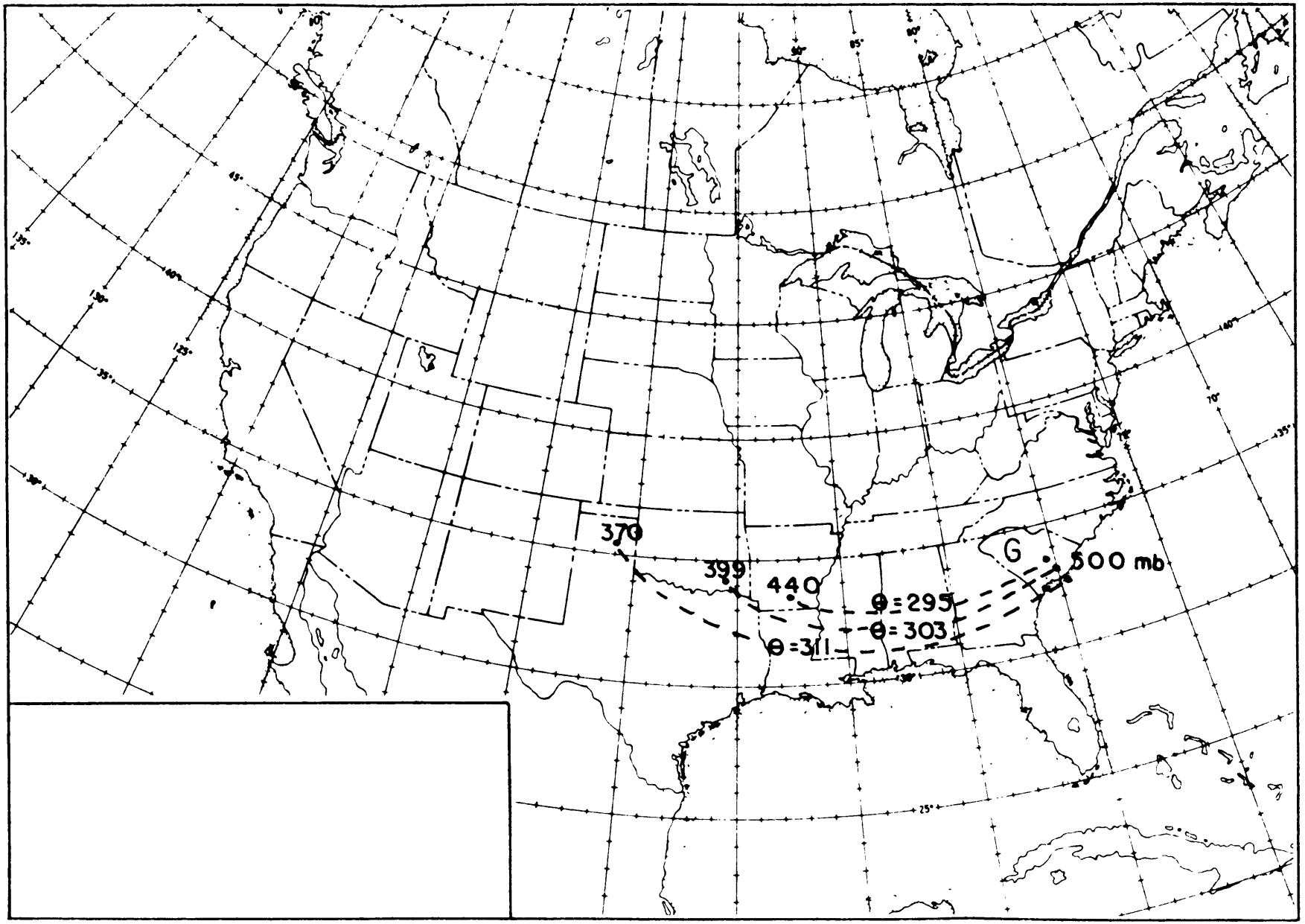

FIGURE 27

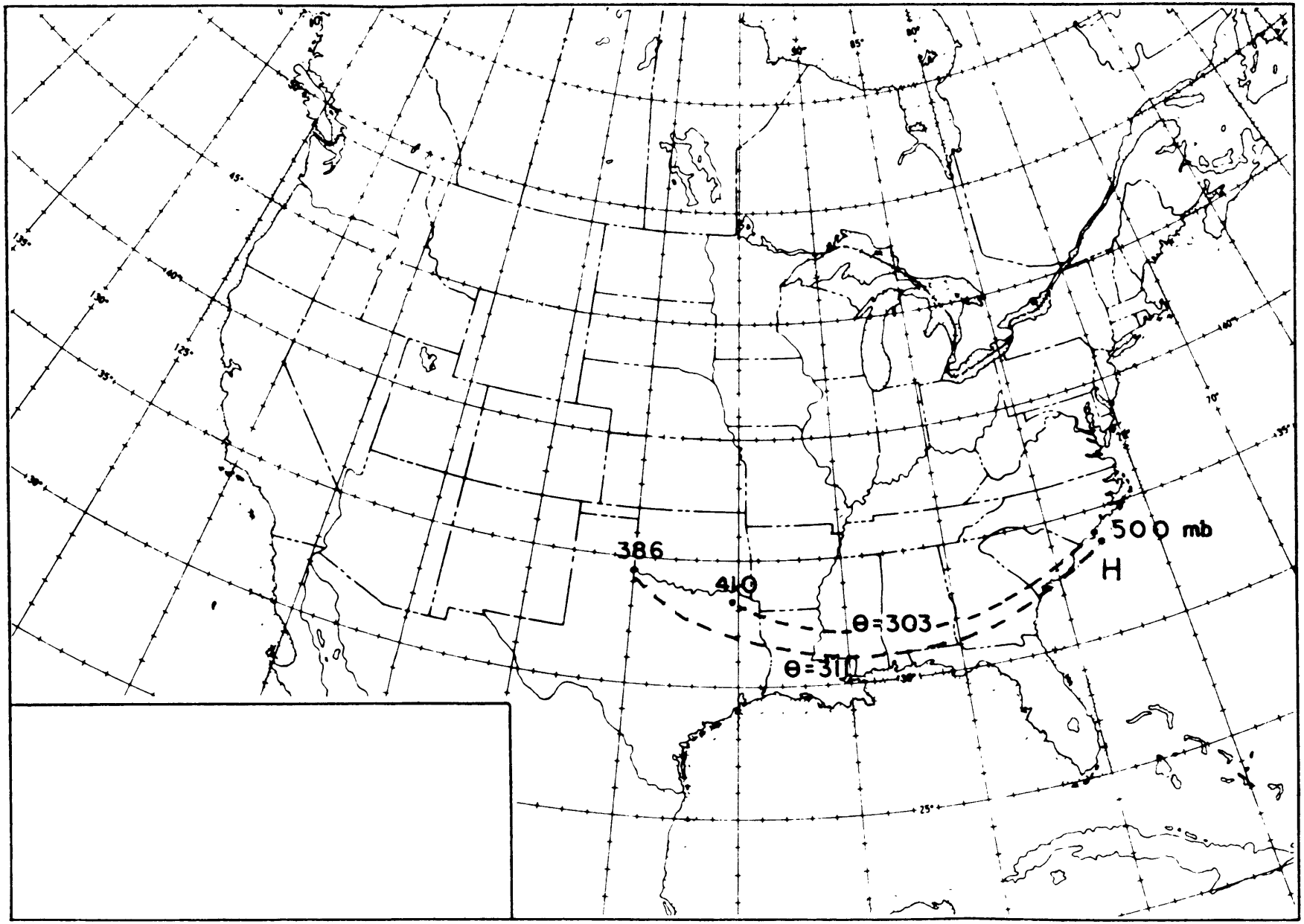

FIGURE 28

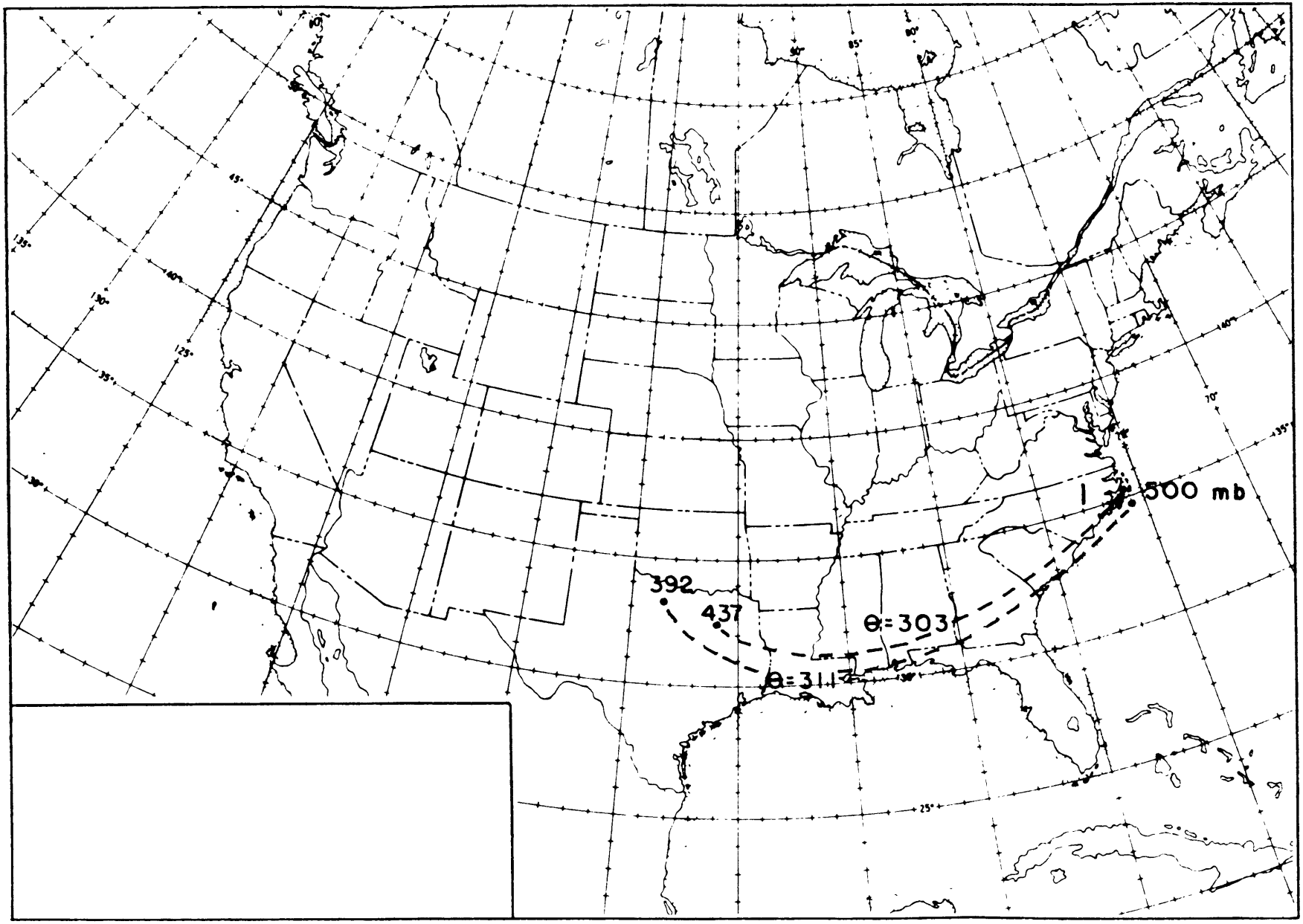

FIGURE 29

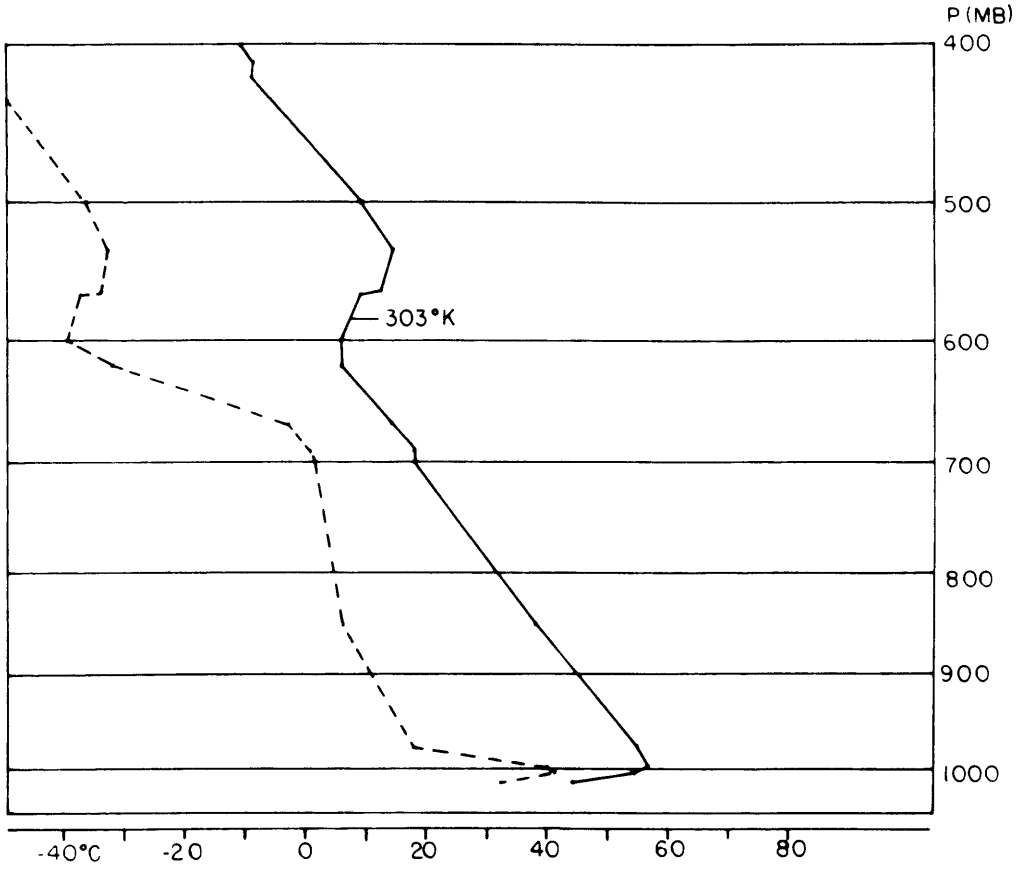

FIGURE 30 CRP — 19 FEB. 1964 1200 GMT

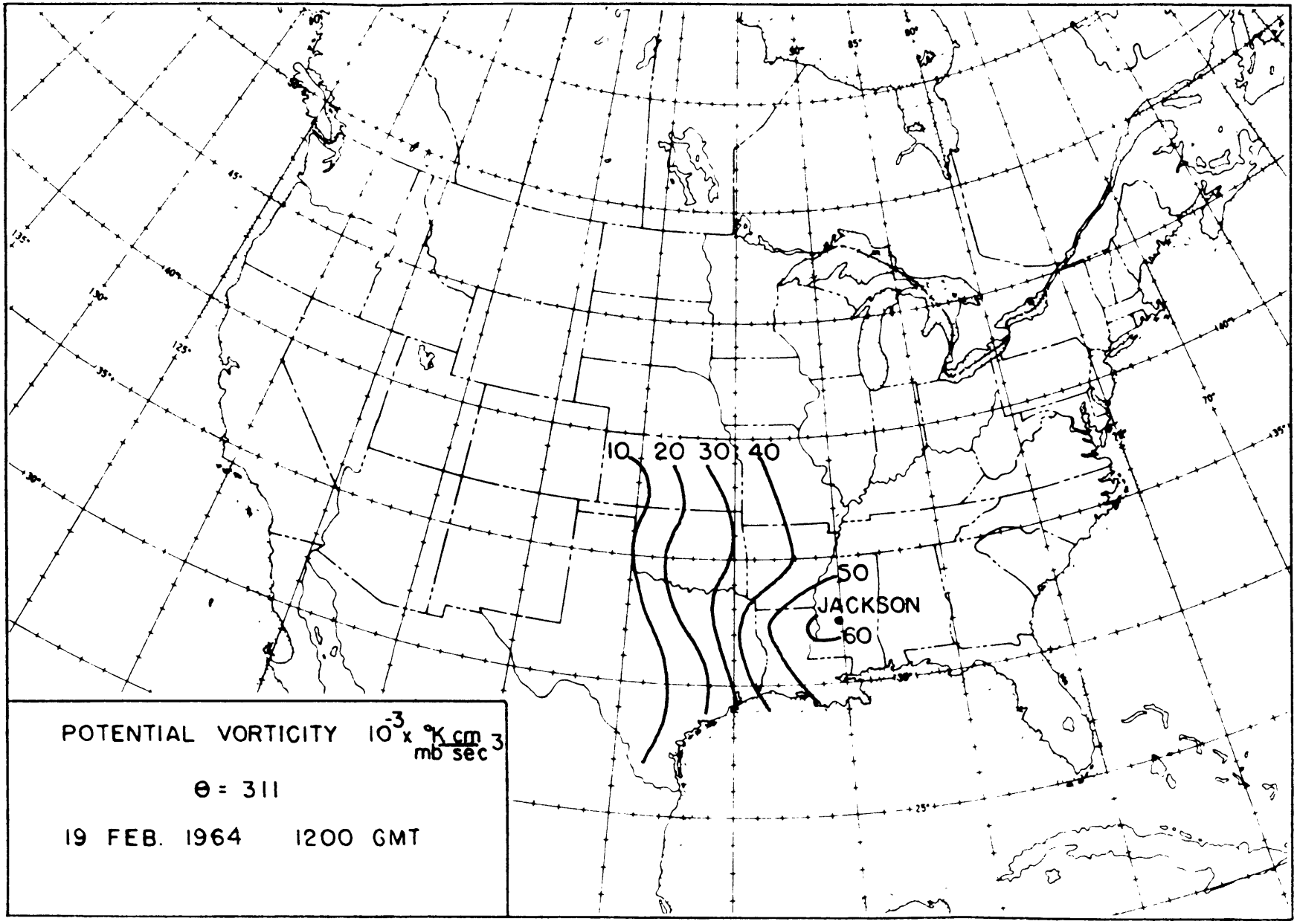
10
20
30
40
50
JACKSON
60
POTENTIAL VORTICITY 10^{-3} x $\frac{°K\ cm^3}{mb\ sec}$
θ = 311
19 FEB. 1964 1200 GMT

FIGURE 31

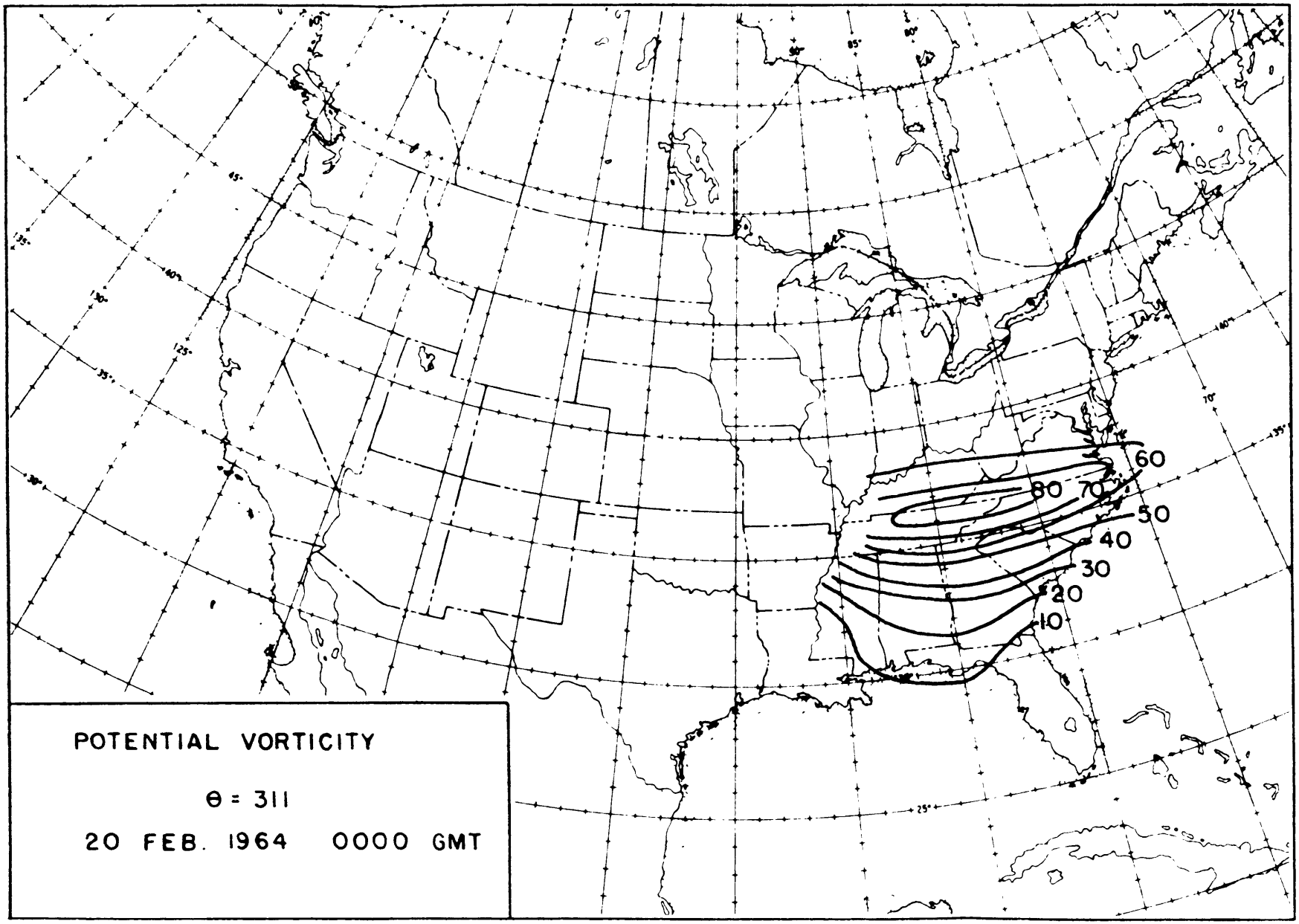
60
80
70
50
40
30
20
10
POTENTIAL VORTICITY
θ = 311
20 FEB. 1964 0000 GMT

FIGURE 32

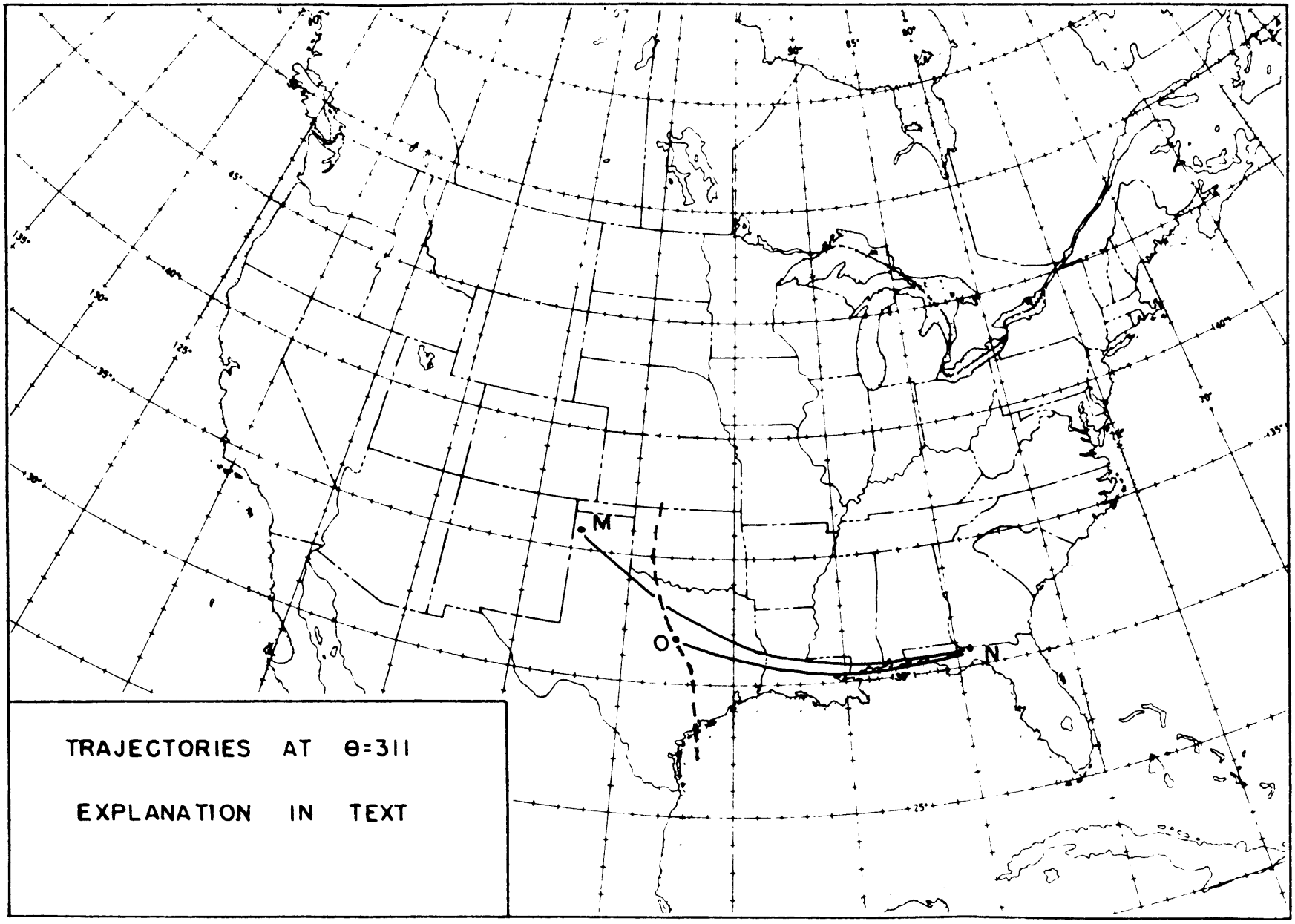

FIGURE 33

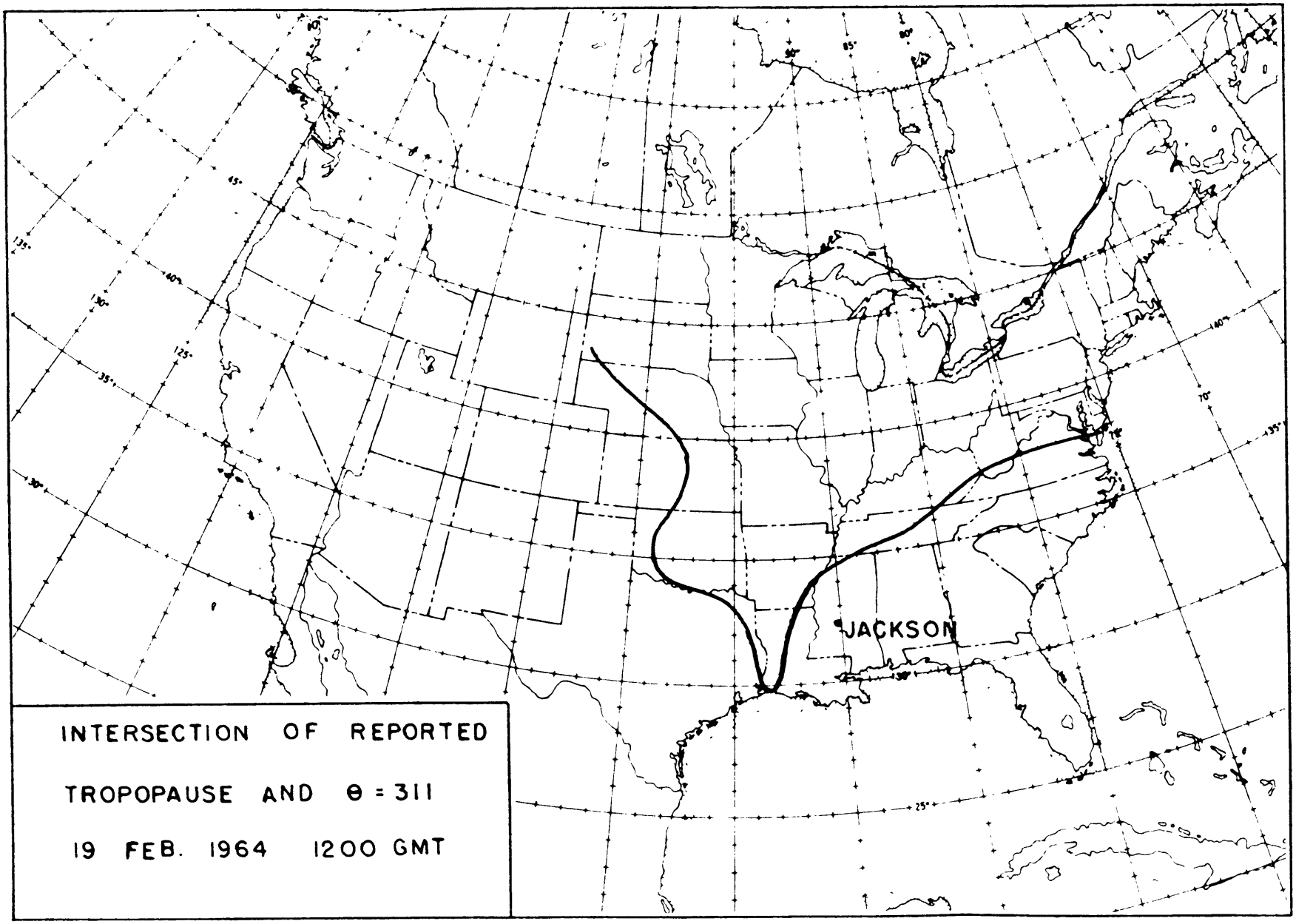
JACKSON
INTERSECTION OF REPORTED
TROPOPAUSE AND θ = 311
19 FEB. 1964 1200 GMT

FIGURE 34

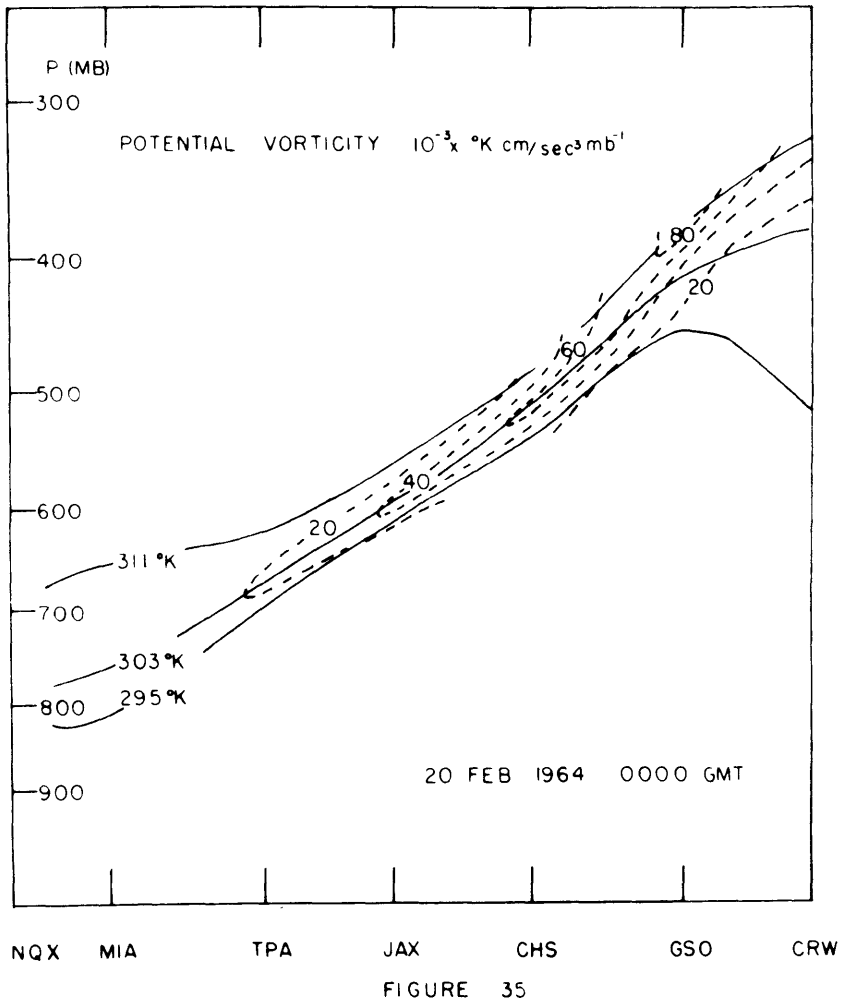
P (MB)
300
400
500
600
700
800
900
POTENTIAL VORTICITY 10^{-3}x °K cm/sec³ mb⁻¹
80
20
60
40
20
311 °K
303 °K
295 °K
20 FEB 1964 0000 GMT
NQX
MIA
TPA
JAX
CHS
GSO
CRW

FIGURE 35

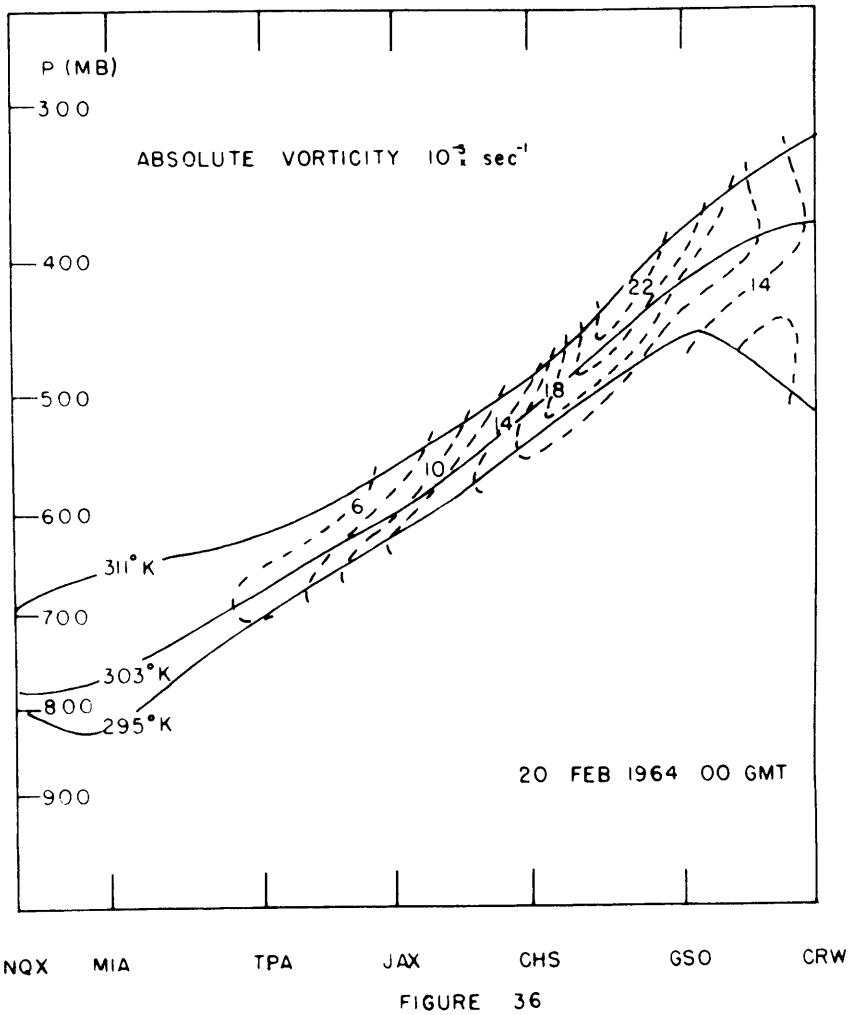
P (MB)
300
400
500
600
700
800
900
ABSOLUTE VORTICITY 10⁻⁵ sec⁻¹
22
14
18
14
10
6
311°K
303°K
295°K
20 FEB 1964 00 GMT
NQX
MIA
TPA
JAX
CHS
GSO
CRW

FIGURE 36

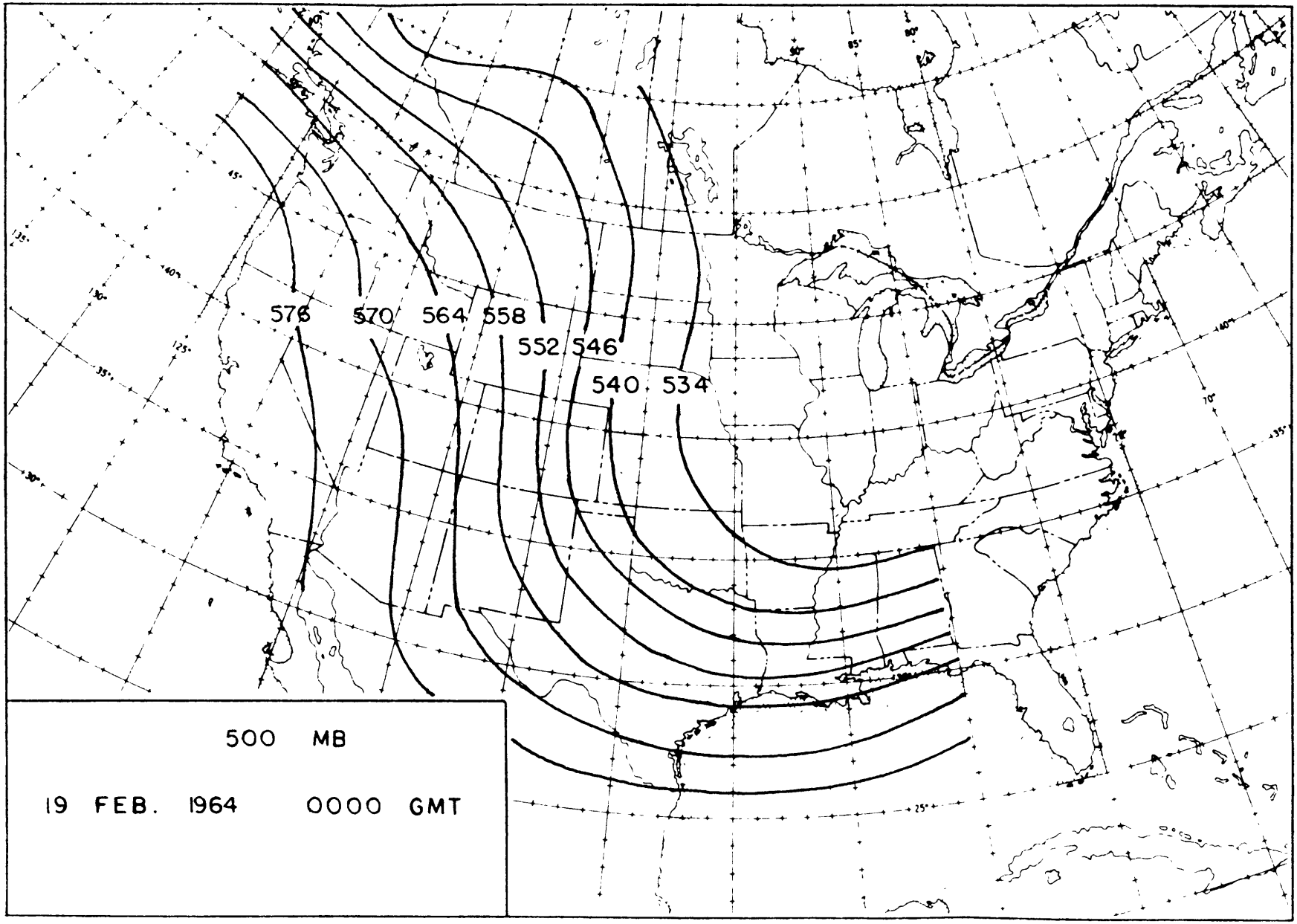

FIGURE 37